NASA/TP—2006–214713

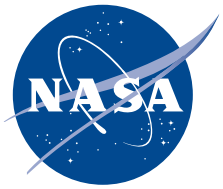

Measuring Core/Facesheet Bond Toughness in Honeycomb Sandwich Structures

A.T. Nettles
Marshall Space Flight Center, Marshall Space Flight Center, Alabama

December 2006

The NASA STI Program…in Profile

Since its founding, NASA has been dedicated to the advancement of aeronautics and space science. The NASA Scientific and Technical Information (STI) Program Office plays a key part in helping NASA maintain this important role.

The NASA STI program operates under the auspices of the Agency Chief Information Officer. It collects, organizes, provides for archiving, and disseminates NASA's STI. The NASA STI program provides access to the NASA Aeronautics and Space Database and its public interface, the NASA Technical Report Server, thus providing one of the largest collections of aeronautical and space science STI in the world. Results are published in both non-NASA channels and by NASA in the NASA STI Report Series, which includes the following report types:

- TECHNICAL PUBLICATION. Reports of completed research or a major significant phase of research that present the results of NASA programs and include extensive data or theoretical analysis. Includes compilations of significant scientific and technical data and information deemed to be of continuing reference value. NASA's counterpart of peer-reviewed formal professional papers but has less stringent limitations on manuscript length and extent of graphic presentations.

- TECHNICAL MEMORANDUM. Scientific and technical findings that are preliminary or of specialized interest, e.g., quick release reports, working papers, and bibliographies that contain minimal annotation. Does not contain extensive analysis.

- CONTRACTOR REPORT. Scientific and technical findings by NASA-sponsored contractors and grantees.

- CONFERENCE PUBLICATION. Collected papers from scientific and technical conferences, symposia, seminars, or other meetings sponsored or cosponsored by NASA.

- SPECIAL PUBLICATION. Scientific, technical, or historical information from NASA programs, projects, and missions, often concerned with subjects having substantial public interest.

- TECHNICAL TRANSLATION. English-language translations of foreign scientific and technical material pertinent to NASA's mission.

Specialized services also include creating custom thesauri, building customized databases, and organizing and publishing research results.

For more information about the NASA STI program, see the following:

- Access the NASA STI program home page at <http://www.sti.nasa.gov>

- E-mail your question via the Internet to <help@sti.nasa.gov>

- Fax your question to the NASA STI Help Desk at 301–621–0134

- Phone the NASA STI Help Desk at 301–621–0390

- Write to:
  NASA STI Help Desk
  NASA Center for AeroSpace Information
  7115 Standard Drive
  Hanover, MD 21076–1320

NASA/TP—2006–214713

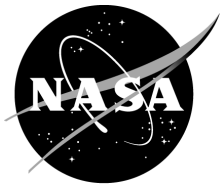

Measuring Core/Facesheet Bond Toughness in Honeycomb Sandwich Structures

A.T. Nettles
Marshall Space Flight Center, Marshall Space Flight Center, Alabama

National Aeronautics and
Space Administration

Marshall Space Flight Center • MSFC, Alabama 35812

December 2006

TRADEMARKS

Available from:

NASA Center for AeroSpace Information
7115 Standard Drive
Hanover, MD 21076–1320
301–621–0390

This report is also available in electronic form at
<https://www2.sti.nasa.gov>

TABLE OF CONTENTS

LIST OF FIGURES

LIST OF FIGURES (Continued)

LIST OF TABLES

LIST OF ACRONYMS AND SYMBOLS

A_C	area under the curve
ASTM	American Society for Testing Materials
a	crack length
a_i	various crack length values
a_{i-1}	original length of the crack
C	specimen compliance
CC	compliance calibration
CD	climbing drum
C_0	first-order compliance constant
D_1	amount of facesheet peeled
D_2	total drum displacement
DCB	double cantilever beam
d	transverse displacement
d/a	transverse displacement divided by crack length
d/P_C	transverse displacement divided by critical load
E_1	flexural modulus of the facing
E_2	flexural modulus of the core with one bonded facesheet
E_T	energy associated with peeling
FWT	flatwise tension
G_{IC}	measure of toughness; critical strain energy release rate

LIST OF ACRONYMS AND SYMBOLS (Continued)

I_1	moment of inertia of the cross section of the facing
I_2	moment of inertia of the cross section of the core with one bonded facesheet
n	constant
P_C	applied load that causes crack growth (critical load)
P_{i-1}	associated load to begin propagation
PVC	polyvinyl chloride
P_1	load to overcome drum rolling up facesheet material
P_2	load to peel facing from core
pcf	pounds per cubic foot
r_1	inner radius of drum + one-half facesheet thickness
r_2	outer radius of drum + one-half strap thickness
T_1	triangle 1
T_2	triangle 2
t_f	thickness of face being peeled
w	specimen width
$w\Delta a_i$	surface area created
Δa_i	a region of crack growth
∂	partial differentation

TECHNICAL PUBLICATION

MEASURING CORE/FACESHEET BOND TOUGHNESS IN HONEYCOMB SANDWICH STRUCTURES

1. INTRODUCTION

Honeycomb sandwich structures will be used in future launch vehicles due to the fact that the strength-to-mass ratio surpasses any other method of construction. Key structural elements will undoubtedly contain sandwich structures and thus be considered fracture critical. Honeycomb core cryogenic fuel tanks for spacecraft have been proposed and these structures will experience large thermal and mechanical loads. The drawback of these structures is usually the core/facesheet bond. The resin that bonds the facesheet to the honeycomb must form fillets that effectively transfer loads from the facesheet to the core. Under mode-I (opening mode), stress on the facesheet can peel away from the honeycomb if not well bonded, and since there are no mechanical fasteners or other crack stoppers, this failure can debond extremely large areas causing catastrophic failure. The X–33 liquid hydrogen tank is a well-publicized case of this type of failure.[1]

A structure as simple as a curved panel, when subjected to loading that tends to flatten-out the panel, induces open-mode stresses. A helicopter landing gear door experienced catastrophic failure when a gust of wind induced open-mode stress into the curved sandwich panel.[2] For a proposed D-shaped cryogenic tank made of honeycomb construction, open-mode stress in the vicinity where the flat and curved sections met was found to be on the order of 1,500 psi when the tank was pressurized to 42 psi and filled with liquid hydrogen.[3] It has also been shown that sandwich panels with a 1-in curvature radius can experience an opening mode stress seven times that of the applied shear stress, which is more than enough to disbond typical aerospace type structures.[4] This curvature radius is close to that seen on many sections of the X–37 fuselage.

The catastrophic nature of a core/skin disbond has not gone unnoted and some efforts have been made to develop peel-stoppers to somewhat contain the amount of disbond. Olsson and Lonno presented a concept in which the upper and lower facesheets are periodically joined with additional facesheet material placed in the core.[5] A more simple approach was taken by Grenestedt, where the facesheet is periodically made discontinuous so if peeling does occur, the facesheet will totally separate and fall off of the structure at the areas where the peel-stoppers are placed.[6] However, it is best to simply have the strongest bond possible to maximize peeling resistance.

It is of utmost importance to maximize both the bond strength and the bond toughness for a sandwich structure. Methods to measure bondline strength and toughness are needed before these parameters can be maximized. The flatwise tension (FWT) test is most often used to measure bondline strength and

is the American Society for Testing and Materials (ASTM) standard number C297. For mode I toughness, however, no standard exists for finding the critical strain energy release rate, a measure of toughness designated by G_{IC}. The climbing drum (CD) peel test, ASTM Standard D1781, exists for quality control and relative comparisons, but is not intended to be used to find a fracture toughness value. Values from the CD peel test are given as a torque per unit width to peel off the facing. In a paper by Okada and Kortschot it was contended that a critical strain energy release rate could be calculated by simply dividing the failure torque by the radius of the drum.[7] Values generated using this method were compared to values obtained using a double cantilever beam (DCB) test and similar values were obtained; however, a solid laminate—not a sandwich panel—was tested. For critical strain energy release rate (G_{IC}) testing of core/facesheet fracture toughness, some experimental methods have been utilized with various data reduction schemes. The most widely used method is the DCB test with a compliance calibration (CC) data reduction technique.

The aim of this study is to examine two basic test techniques to assess the G_{IC} of a honeycomb sandwich bondline, then compare and discuss the results. The two basic test techniques to be used are: (1) DCB using two methods of data reduction, and (2) CD peel.

The only variations in the specimens will be in the facesheet thickness (and thus stiffness) and core density, since these variables can influence most of the tests for a given material system.

2. BACKGROUND

Mode I critical strain energy release rate of skin/core bonds have been tested and studied before. Most of these studies followed the general outline for determining the critical strain energy release rate of a composite laminate, which is given in ASTM D5528, with adaptations for the honeycomb core. Some of these cores were foam and not honeycomb, but the same basic testing techniques are applicable. In a study using aluminum facings bonded to polyvinyl chloride (PVC) foam cores the DCB method was used to find G_{IC} values.[8] A number of different methods are available to reduce the data to obtain G_{IC} values. In this study a CC procedure based on the following equation was used:

$$G_{IC} = \frac{P_C^2}{2w}\frac{\partial C}{\partial a} \quad , \tag{1}$$

where,

G_{IC} = critical strain energy release rate

P_C = applied load that causes crack growth (critical load)

w = specimen width

C = specimen compliance = d/P_C where d = transverse displacement

a = crack length

The experimentally determined compliance versus crack length data was fitted to a power curve as

$$C = C_0 a^n \quad . \tag{2}$$

Differentiating, with respect to crack length, makes equation (1) become

$$G_{IC} = \frac{P_C^2}{2b} n C_0 a^{n-1} \quad . \tag{3}$$

This is the governing equation used to find the critical strain energy release rate as a function of critical load, displacement, and crack length.

The data from this experimental program indicated that the DCB test used on sandwich specimens yielded valid critical strain energy release rates. Introduction of the loads into the panel was via hinges at the specimen ends, as illustrated in figure 1, which is very common for DCB testing.

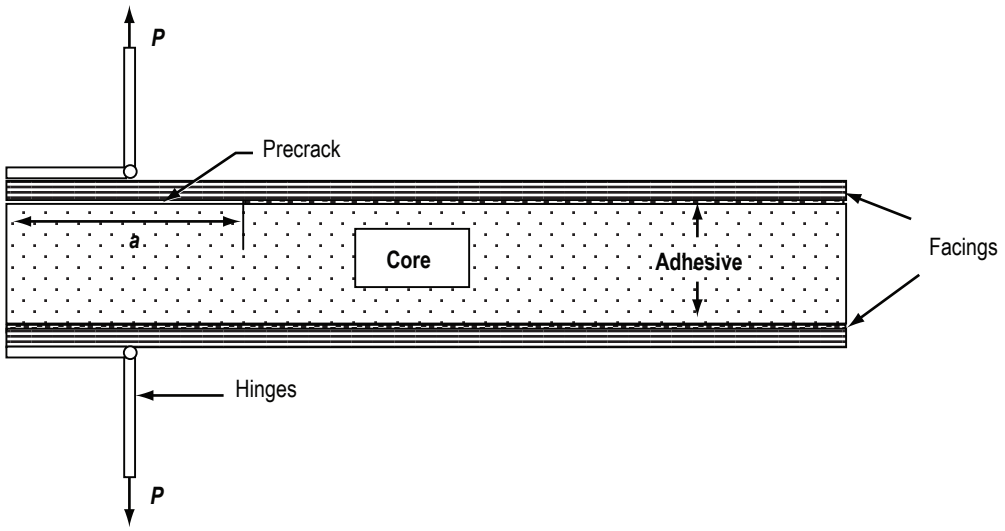

Figure 1. DCB test schematic used in reference 8.

In another experimental program using balsa and foam cores (no honeycomb), a similar data reduction methodology was used, but only single cantilever beam specimens were tested.[9] This consists of bonding the sandwich specimen to a sliding carriage and peeling the top facesheet as in a DCB test. In this study the "areas method" was also used to calculate the critical strain energy release rate. This method simply involves calculating the area under the load-displacement curve and dividing this by the resulting surface area created due to the peeling. The data indicated that the areas method tended to give higher critical strain energy release rates compared to the CC method. Some CD peel tests were also performed. It was mentioned in this Technical Publication (TP) that one of the limiting factors in utilizing the CD peel test is the thickness of the facesheets. If the facesheets are too thick then they will not wrap around the drum and thus the cantilever beam test must be utilized. A qualitative measurement of the two methods showed that as the critical strain energy release rate increased, the climbing peel torque also increased, as expected. However, a quantitative analysis shows that the CD peel test yields a lower value (approximately 1/3) of critical strain energy release rate for a given type of sandwich panel. For lightweight foam cores, it was found that the precrack between the core and facesheet would propagate into the core and not along the core/facesheet interface.

Another study used the DCB test to evaluate the effects of facesheet thickness.[10] Instead of using a CC method, a linear beam analysis was used leading to the following equation:

$$G_{IC} = \frac{P_C^2 a^2}{2w}\left[\frac{1}{E_1 I_1} + \frac{1}{E_2 I_2}\right] \tag{4}$$

where,

G_{IC} = critical strain energy release rate

P_C = critical load

w = specimen width

a = crack length

E_1 = flexural modulus of the facing

I_1 = moment of inertia of the cross section of the facing

E_2 = flexural modulus of the core with one bonded facesheet

I_2 = moment of inertia of the cross section of the core with one bonded facesheet.

It should be noted that these equations are only valid for small deflections, indicating that very stiff facesheets need to be present and that the crack length cannot be large. This experimental procedure was unique because instead of using hinges at the beam ends, wires were wrapped around each facesheet and pulled on, as illustrated in figure 2.

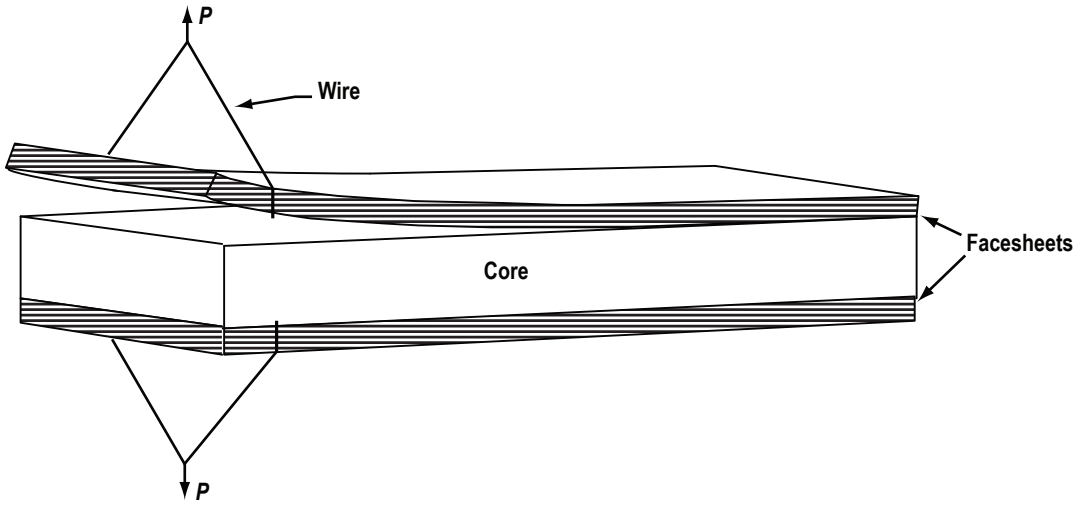

Figure 2. Using wires instead of hinges on a DCB specimen.

If the facesheets are relatively thin, it may be necessary to bond stiffeners to them to perform a DCB test, as in a study on high-temperature testing.[11] For this study, steel plates were mechanically fastened to the facesheets, since adhesives fail at high temperatures, and the classic CC method was used for data reduction. It was found that the R-curves (G_{IC} versus crack length plots) showed a trend of decreasing G_{IC} values with increasing crack length.

In at least one study, a precrack was made on both core/facing bondlines and a DCB test was performed.[12] The limitations of nonlinear stress-strain curves are explained and a number of data reduction schemes are used to find G_{IC}. The author also makes the argument that most errors in G_{IC} measurements arise from inaccurate crack length measurements, especially on wider specimens where the crack length may not be the same on both sides.

The power-law fit, mentioned in reference 8, was used in a study of carbon/epoxy facesheets bonded to Nomex honeycomb core.[13] This power-law fit was then used to imply crack length once enough data had been collected to generate a good fit for a given specimen. The resulting equation is

$$G_{IC} = \frac{P_C^2}{2w} n C_0 \left[\left(\frac{d}{P_{C_0}} \right)^{1/n} \right]^{n-1} . \tag{5}$$

Equation (2) is used to find the constants n and C_0. It was found in this study that the R-curve was essentially flat (i.e. G_{IC} was independent of crack length).

Techniques other than the CD peel, the DCB, and the single cantilever beam that have been used to find G_{IC} for a core/facesheet bond include the facesheet push-off test and the modified three-point bend.[14,15]

3. ANALYSIS

3.1 Climbing Drum

It was stated in reference 7 that the critical strain energy release rate can be determined from a CD peel test by dividing the peel torque by the radius of the drum. Examining the mechanics of the CD peel test can give a relation between displacement and length of peeled facesheet. Figure 3 defines the notation that will be used.

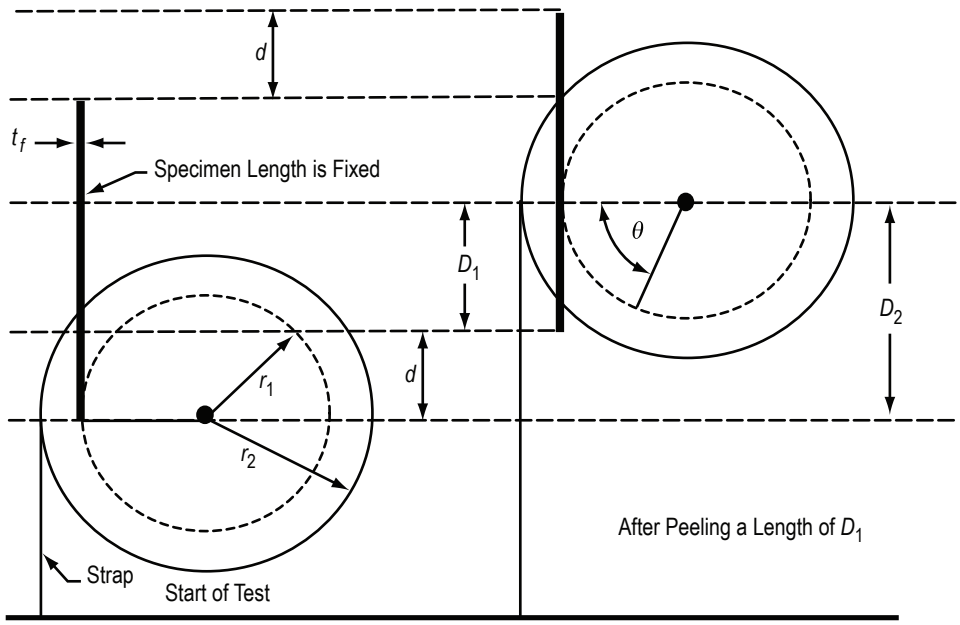

Figure 3. Schematic of CD peel test at start (left) and after peeling a length (D_1) of facesheet (right).

The following notation is used in figure 3:

d = load frame displacement

t_f = thickness of facing being peeled

r_1 = inner radius of drum + one-half facesheet thickness

r_2 = outer radius of drum + one-half strap thickness

D_1 = amount of facesheet peeled

D_2 = total displacement of drum

θ = angle through which drum rotates.

It can be seen from figure 3 that

$$D_2 = D_1 + d \ . \tag{6}$$

Since the arc length of a circle segment is given by r_θ then,

$$D_2 = r_2\theta \ \text{ and } \ D_1 = r_1\theta \ . \tag{7}$$

Substituting the second part of equation (7) into the first part gives

$$D_2 = \frac{r_2}{r_1} D_1 \ , \tag{8}$$

and putting equation (8) into equation (6) gives

$$D_1 = \frac{r_1 d}{r_2 - r_1} \ , \tag{9}$$

which is the amount of facesheet peeled as a function of displacement and the radii of the drum. A schematic of CD peel load versus displacement is shown in figure 4.

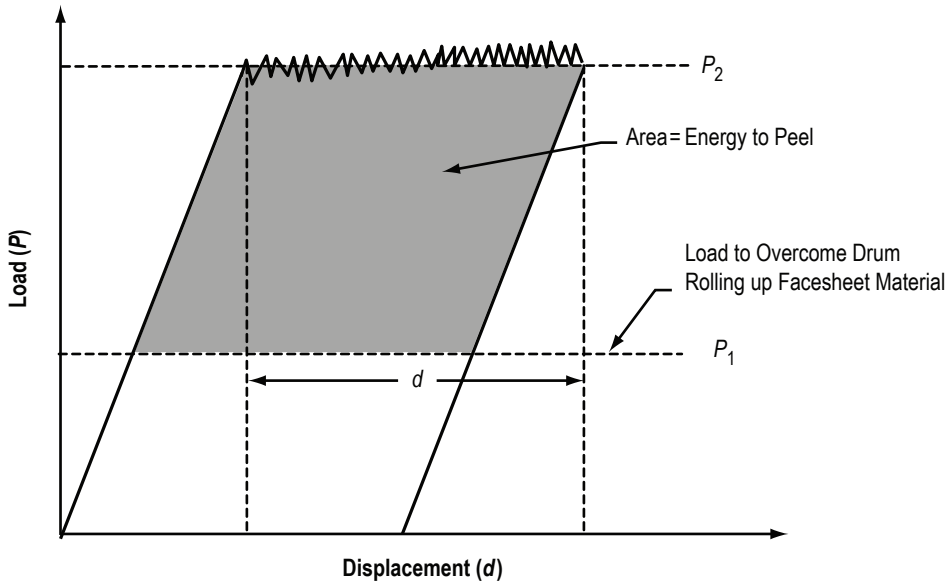

Figure 4. Schematic of CD peel test data.

It can be seen that the energy to peel is the area of the parallelogram under the curve between P_1 and P_2. Dividing this area by the surface area created on the peel specimen gives the critical strain energy release rate

$$G_{IC} = \frac{(P_2 - P_1)d}{wD_1} \quad , \tag{10}$$

where w = specimen width, and putting equation (9) into equation (10) gives

$$G_{IC} = \frac{(P_2 - P_1)d(r_2 - r_1)}{w_{r_1} d} = \frac{(P_2 - P_1)(r_2 - r_1)}{w_{r_1}} \quad . \tag{11}$$

Equation (11) is the peel torque divided by r_1. In theory, this is the critical strain energy release rate as determined from a CD peel test.

3.2 Double Cantilever Beam

It can be seen from the references, that a number of methods exist for reducing the data to obtain a critical strain energy release rate. The most common are all based on equation (1), which was given in the introduction as

$$G_{IC} = \frac{P_C^2}{2w} \frac{\partial C}{\partial a} \quad , \tag{12}$$

where

G_{IC} = critical strain energy release rate

P_C = critical load

w = specimen width

C = specimen compliance = d/P_C where d = transverse displacement

a = crack length.

Since $C = C_0 a^n$, a plot of compliance versus crack length can be made, and the constants C_0 and n can be found by a curve fit.

Alternatively, since C is defined as d/P_C and is a function of crack length (a), equation (2) can be substituted into equation (1) which will give equation (3). Equation (3) can be written as

$$G_{IC} = \frac{P_C^2}{2w}\frac{nC_0a^n}{a} \quad . \tag{13}$$

Now, equation (2) can be rearranged to give

$$a^n = \frac{C}{C_0} \quad . \tag{14}$$

Putting equation (13) into equation (12) will yield

$$G_{IC} = \frac{P_C^2}{2w}\frac{nC}{a} \quad , \tag{15}$$

and substituting the definition of C will give

$$G_{IC} = \frac{nP_Cd}{2wa} \quad . \tag{16}$$

This is another way of expressing equation (1), which contains only one experimentally determined constant (n) that will still need to be found experimentally from a curve fit. It should be noted that this data reduction technique may produce errors if large displacements are present, since it is based on linear beam theory.

Energy methods can also be used to find the strain energy release rate. Figure 5 is a typical data schematic showing four intervals, a region of crack growth (Δa_i) characterized by the original length of the crack (a_{i-1}), and an associated load to begin propagation (P_{i-1}).

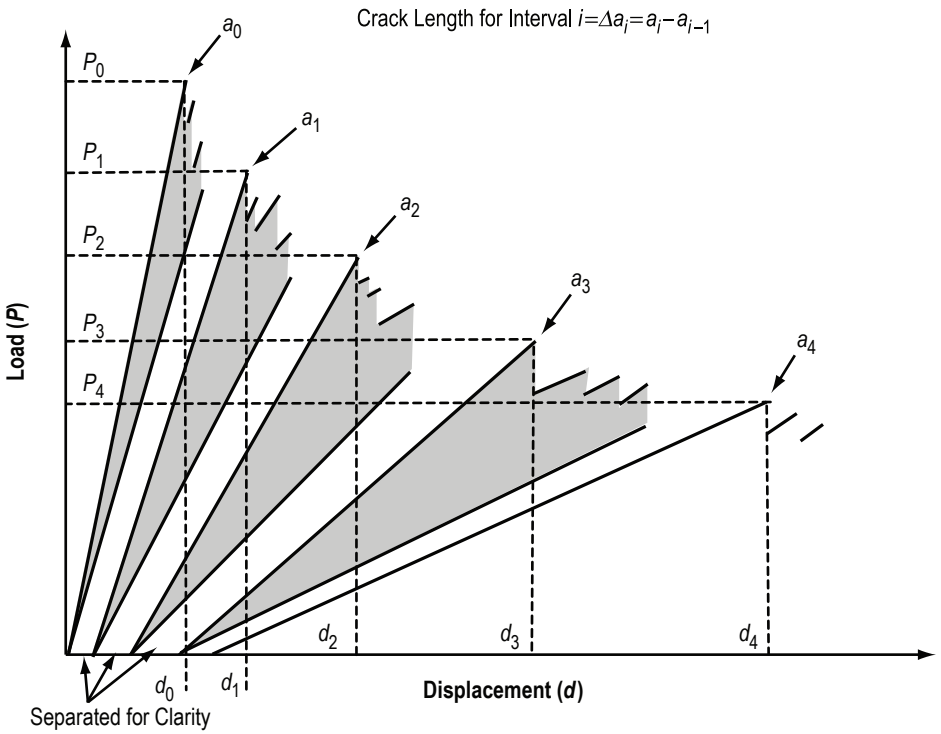

Figure 5. Typical load-displacement data from a DCB test.

The shaded area under the curve representing energy can be calculated and when divided by the surface area created ($b\Delta a_i$) gives a critical strain energy release rate for that particular portion of crack growth. The total shaded area under the curve can be divided by the total amount of surface area created to arrive at an approximate G_{IC} value for the entire specimen. The advantage of utilizing this technique is that it is independent of large deflections.

4. EXPERIMENTAL

4.1 Material Used

Sandwich panels having a 0.5-in thick glass/phenolic core were used for all testing. The two core densities used were 4 ft/lb^3 and 8 ft/lb^3 and both had a 3/16-in cell size. The facesheets consisted of carbon/epoxy plain weave prepreg at 1-, 2-, 3-, 4-, 5-, or 8-plies thick. A 300-g/m^2 areal weight epoxy film adhesive was used between the facesheets and core. The sandwich panels were processed in a platen press as square 14-in panels from which specimens could be cut.

4.2 Climbing Drum Peel Testing

Test specimens measured 12-in long by 3-in wide. One inch was removed from the top of the facesheet and core for gripping. Two inches were removed at the bottom of the specimen and a 3-in long precrack was started, resulting in the specimen shown in figure 6.

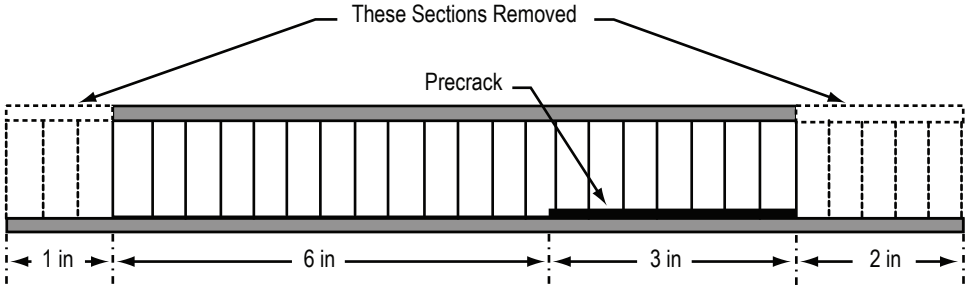

Figure 6. Schematic of CD peel specimen.

The CD peel apparatus was based on ASTM Standard D1781. Originally a commercial fixture was used exactly like that shown in ASTM D1781. For this study, however, a fixture was made that had basically the same dimensions as the commercially available one, but improvements were made that provided easier testing. Figure 7 is a photograph of the fixture used in this study.

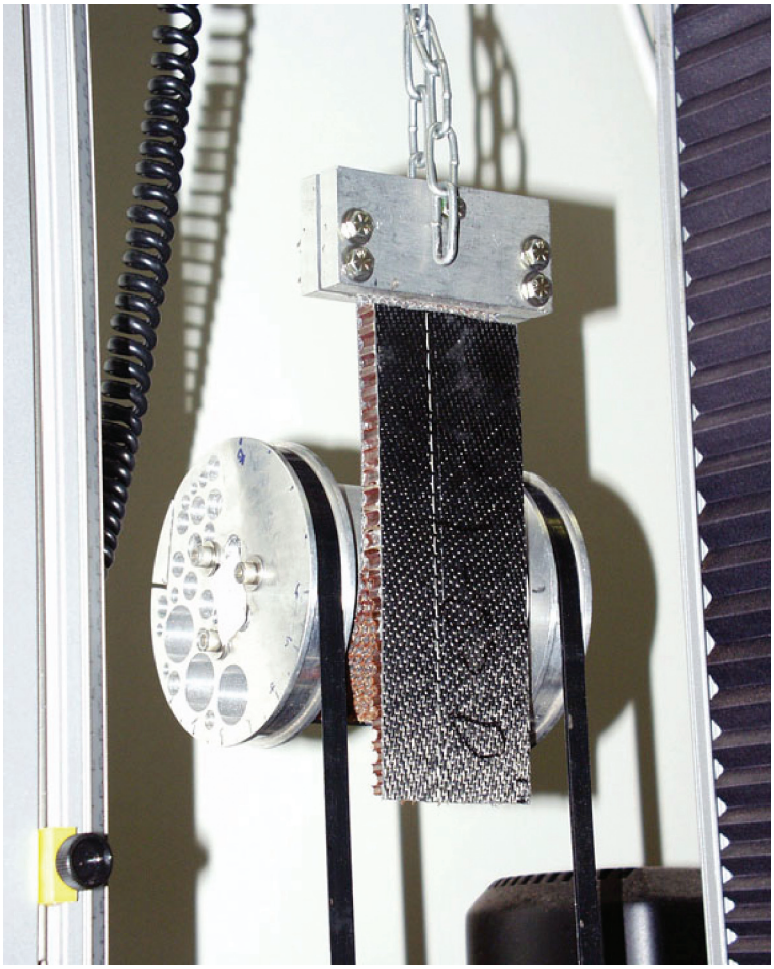

Figure 7. Photograph of CD fixture used in this study.

The commercial fixture used a serrated roller recessed into the drum to grip the specimen. While this did effectively hold the specimen, the facesheet folded over a 90˚ angle before rolling smoothly up the drum causing the facesheet to snap, as shown in figure 8. A schematic of the new method to grip the specimen to the drum is also shown in figure 8. This new method allows a smooth transition of the facesheet from the grip up onto the drum.

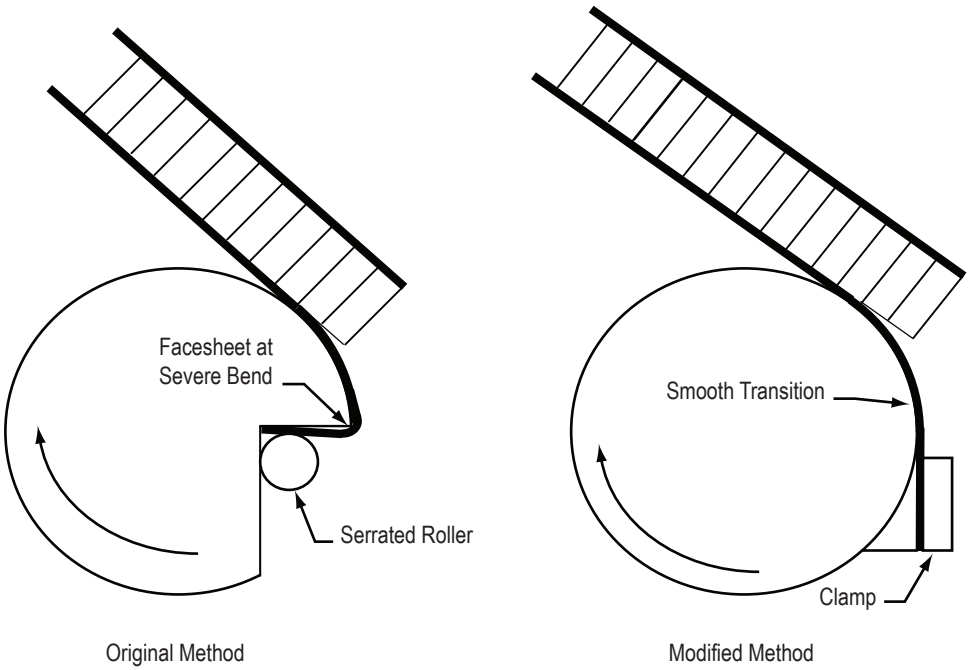

Figure 8. Schematic showing both the old and new method to grip specimen to drum.

The original method to clamp the top part of the specimen consisted of dual serrated rollers that gripped the facesheet by a wedge action. This usually held the specimen; however, it was sometimes difficult to obtain a flat, smooth surface when removing the honeycomb during specimen preparation. In these instances, the upper grip would slip at the beginning phases of the test and the specimen and drum would come crashing down. Instead of using wedge-action grips that hold tighter as the tensile load increases, the modified method preclamped the upper part of the specimen very tightly between two plates so the maximum grip was held throughout the test, even at the beginning.

The 3-in long precrack was used to obtain the load needed to roll up the facesheet and raise the drum. This was subtracted from the total maximum load to determine the load needed to peel the facesheet from the core. A schematic of typical data is shown in figure 9.

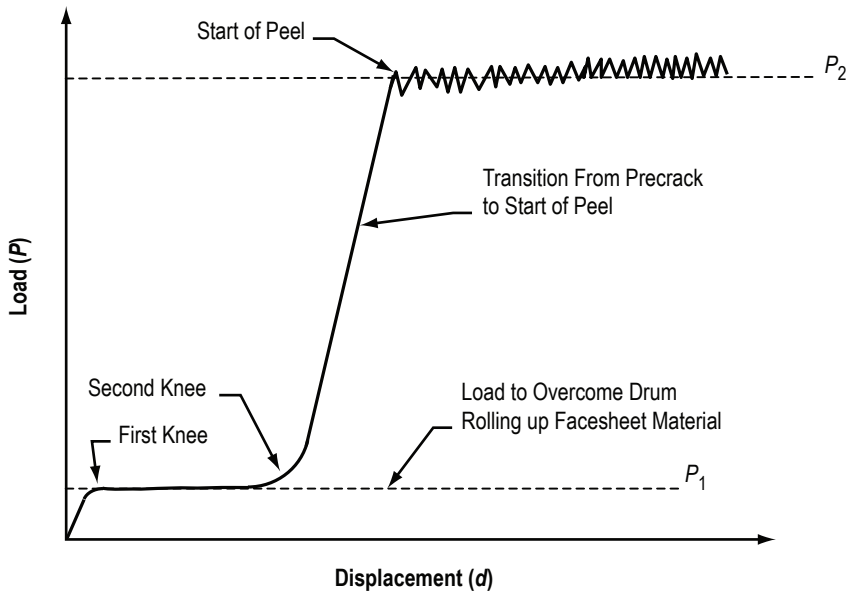

Figure 9. Typical load-displacement data from a CD test.

The value for P_1 was found using an average of all the data from the first knee in the curve to the second knee. The value for P_2 was found using an average of all the data from the start of the peel to the end of the test. The critical strain energy release rate was found from equation (11). The constants of the drum used were

$r_2 = 2.52$ in

$r_1 = 2$ in + $t_f/2$, where t_f is the thickness of the facesheet being peeled.

4.3 Double Cantilever Beam Testing

DCB tests were conducted using two methods. The first method involved bonding stiffening plates with mechanically attached loading blocks to the sandwich specimen. In the second method, the facesheets were loaded from their inner surfaces, as described in reference 10.

Test specimens measured 6.5-in long by 2-in wide. For the first series of tests, the specimens were bonded to 0.25-in thick aluminum plates with mechanically attached loading blocks. This solved the previous problem of hinges directly bonded to the facesheets popping off or breaking during the test. A drawing of the test specimen is shown in figure 10.

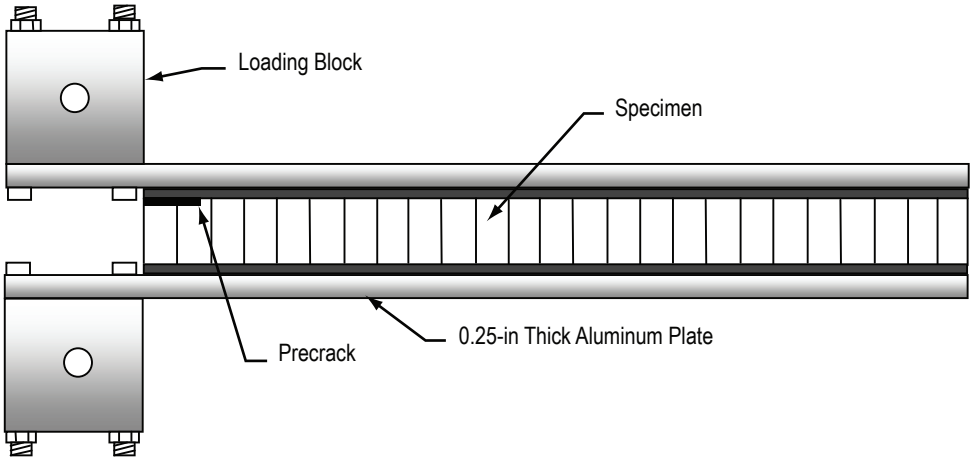

Figure 10. Specimens used for first series of DCB tests, referred to as stiffened specimens.

To better see the crack growth, an edge of the specimen was filled with spackling compound that provided a smooth surface from the facesheet to the core. The core/facesheet interface was then painted with white or yellow tempera paint, which is very brittle and provides an excellent view of the crack front. A photograph of the test setup and a closeup view of the crack front are shown in figure 11.

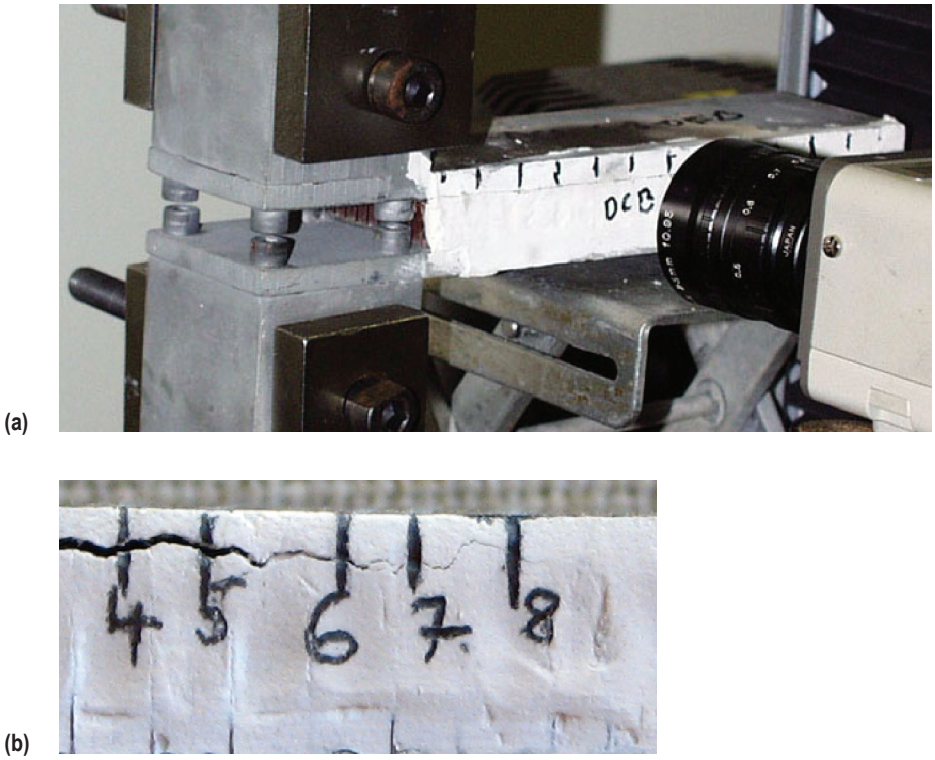

Figure 11. Photograph of (a) the first series of DCB tests and (b) a closeup of crack growth.

It was found that the crack growth tended to jump in discreet increments due to the nature of the honeycomb/facesheet bond. This stick-slip behavior has also been observed in another study.[7] Therefore, instead of marking off the specimen in increments before testing, a mark was put at the crack front on the specimen after a discreet growth event and the test was paused and then unloaded. The loading would then begin again for the specimen with the new, longer crack length. The marks on the specimen were measured after the entire test was completed to obtain the various crack length values (a_i).

For the second series of tests, no stiffeners were bonded to the specimens. The specimens had four bolts mechanically attached to them so they could be loaded from the inside of the facesheets to eliminate hinges. This was done to see if artificially stiffening the facesheets would affect the fracture toughness values. A drawing of the test specimen is shown in figure 12. An edge of the specimen was filled with spackling compound and painted like the first series of DCB tests. A photograph of the test setup for the second series of DCB tests is shown in figure 13.

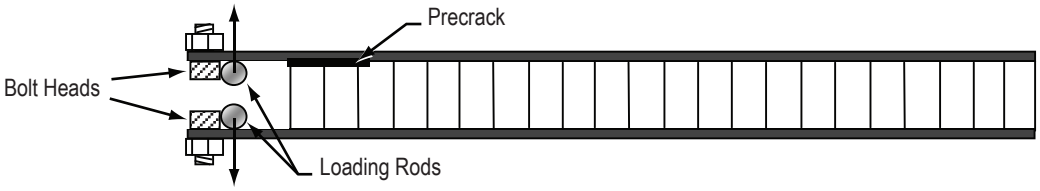

Figure 12. Specimens used for the second series of DCB tests, referred to as nonstiffened specimens.

Figure 13. Photograph of the second series of DCB tests.

5. RESULTS

5.1 Climbing Drum Peel Tests

Results from the CD peel testing demonstrated consistent fracture toughness values for the material system tested in this report. Figure 14 is a typical load-displacement curve from a test showing the load needed to roll up the facesheet is 14.7 lb and the load needed to peel the facesheet is 101.1 lb. This gives a delta load of 86.4 lb. From equation (11) this gives a 7.2-in·lb/in^2 critical strain energy release rate.

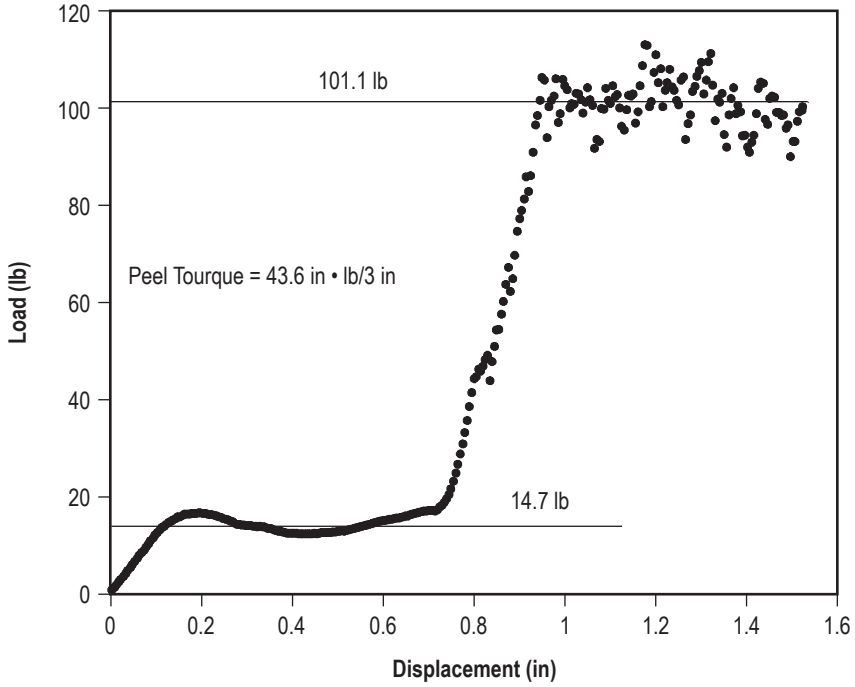

Figure 14. Typical data from a CD peel test.

Sandwich panels were tested with facesheets made of 2, 3, 4, and 5 plies of woven carbon/epoxy prepreg. About half of the CD tests were performed with specimens having a glass/phenolic core density of 4 lb/ft^3 and the other half with a core density of 8 lb/ft^3. Most of the tests were performed by peeling the facesheets in the core ribbon (L) direction while some of the specimens with the 8-lb/ft^3 core had the facesheets peeled in the W direction. Table 1 summarizes the results of the CD peel tests. Appendix A shows the plots used for these data, along with the load to roll up the facesheet and the load to peel. The load to roll up the facesheet may vary for similar facesheets depending on when the apparatus was zeroed out in the load frame. This does not affect the change in load, which is the number needed.

Table 1. Results of CD peel tests.

Specimen ID	Facing Thickness (Plies)	Core Density (p.c.f.)	Pull Direction	Peel Tourque (in•lb/3in)	G_{IC} (in•lb/in^2)
CD7–15–05A	2	4	L	44.3	7.3
CD7–16–05A	3	4	L	47.4	7.9
CD7–16–05B	3	4	L	46.7	7.8
CD7–16–05C	3	4	L	42	7
CD7–18–05NVA	2	4	L	45.9	7.7
CD7–18–05NVB	2	4	L	45.2	7.5
CD7–18–05NVC	2	4	L	46.8	7.8
CD7–18–05VA	2	4	L	45.9	7.7
CD7–18–05VB	2	4	L	44.9	7.5
CD7–18–05VC	2	4	L	46.9	7.8
CD7–20–05A	5	4	L	42.8	7.1
CD7–20–05B	5	4	L	46.5	7.8
CD7–26–05A	2	8	L	42.9	7.2
CD7–26–05B	2	8	L	33	5.5
CD7–26–05C	2	8	L	43.6	7.3
CD7–27–05A	3	8	L	42.8	7.1
CD7–27–05B	3	8	L	47.5	7.9
CD7–27–05C	3	8	L	44.5	7.4
CD7–28–05A	4	8	L	47.8	8
CD7–28–05B	4	8	L	38.3	6.4
CD7–28–05C	4	8	L	42.5	7.1
CD7–28–05–1A	2	8	W	48.7	8.1
CD7–28–05–1B	2	8	W	47.6	7.9
CD7–28–05C–1C	2	8	W	49.5	8.3
CD7–29–05–1A	3	8	W	45.8	7.6
CD7–29–05–1B	3	8	W	43.1	7.2
CD7–29–05–1C	3	8	W	45.1	7.5
CD7–29–05–2A	4	8	W	40.1	6.7
CD7–29–05–2B	4	8	W	46.3	7.7
CD7–29–05–2C	4	8	W	42.7	7.1

From a cursory examination of table 1, it appears that the critical strain energy release rate is independent of core density and number of facesheets. The direction of pull, L or W, also seems to have little effect in the measured values. An obvious outlier was specimen CD7–26–05B, in which the measured strain energy release rate was abnormally low. No known factors could be attributed to this low value. A plot of critical strain energy release rate versus number of facesheets is shown in figure 15 for the data in table 1. For each specimen type, the values used are an average of the tests performed on a panel with a given density core, number of facesheets, and pull direction. The data from specimen CD7–26–05B has been removed.

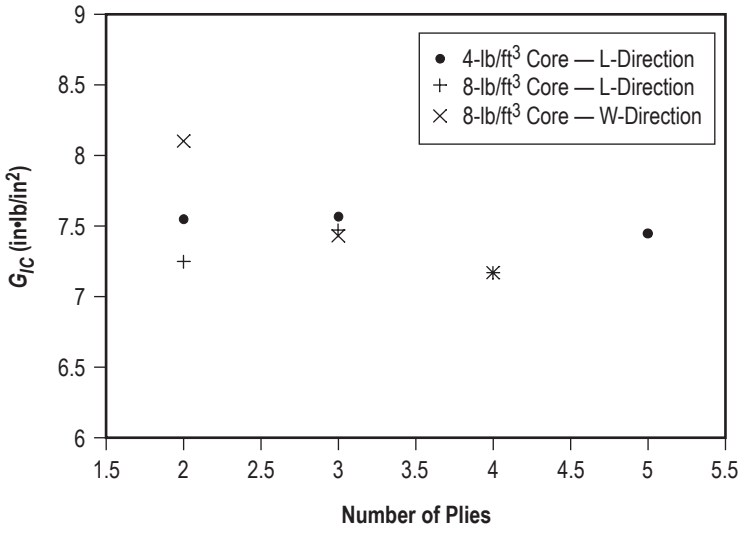

Figure 15. Critical strain energy release rate as a function of the number of facesheet plies for the CD peel tests.

The data are well grouped, and an average of all of the data gives a 7.5-in·lb/in^2 critical strain energy release rate. This will be the value used for comparison with the DCB tests.

5.2 Double Cantilever Beam Tests

Results from the DCB testing showed that there was a distinct difference between the two DCB methods used. For the first series of tests, stiffening plates were bonded to the specimen as described in the experimental section earlier.

5.2.1 Specimens With Stiffening Plates

For specimens that had a honeycomb core of 4-lb/ft^3 density, it was found that the delamination did not propagate at the facesheet/core interface, but rather in the center of the core as shown in figure 16, therefore, only specimens with 8-lb/ft^3 density were tested. A typical load-displacement curve from this type of test, with 8-lb/ft^3 density core is shown in figure 17.

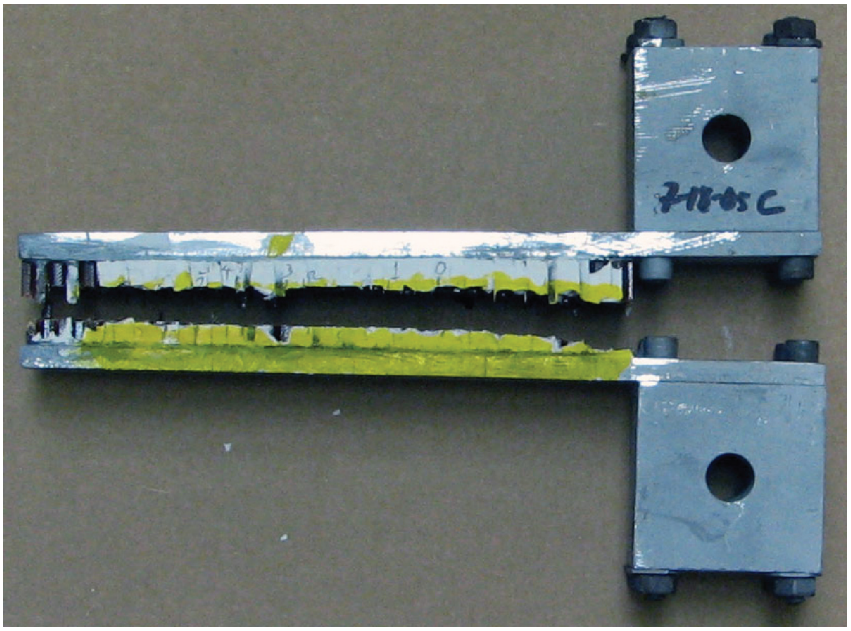

Figure 16. Stiffened DCB specimen with 4-lb/ft^3 core density showing failure in the center of the core material.

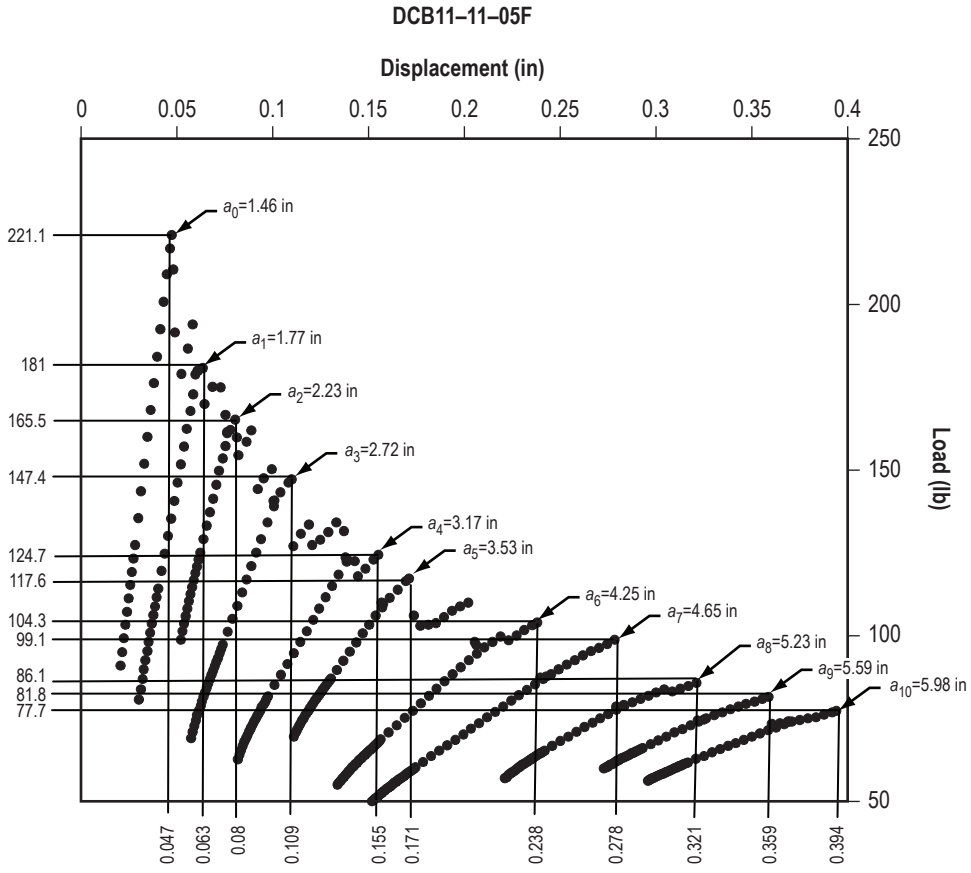

Figure 17. Typical load-displacement data from the first series of DCB stiffened tests.

The data used to determine the critical strain energy release rate are shown on the plot in figure 18. Equations (2) and (3) were used to find the critical strain energy release rate. First, a plot of compliance versus crack length is made and a power law is fit to it. The data of specimen DCB11–11–05F is shown in figure 18. The power-law fit gives constants of C_0=0.000086 (in·lb/in^n) and n=2.27 for equation (2). Equation (3) will thus become

$$G_{IC} = \frac{P_C^2}{2(2\text{in})} 2.27 \left(0.000086 \frac{\text{in}}{\text{lb} \cdot \text{in}^{2.27}} \right) a^{1.27} \quad . \tag{17}$$

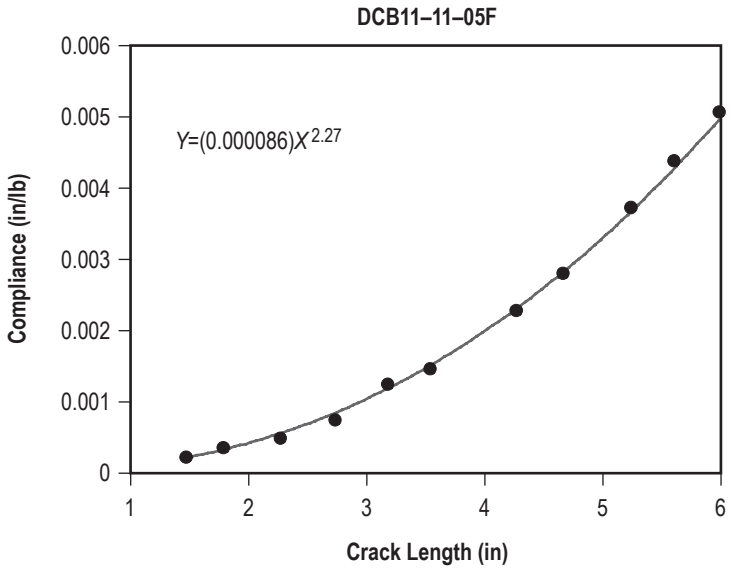

Figure 18. Compliance versus crack length with a power-law fit.

Using the values in figure 17 for the measured loads and associated crack lengths gives an average G_{IC} value of 3.3 in·lb/in^2 for all 11 data points. The R-curve for the data is shown in figure 19.

The curve exhibits a reduction in G_{IC} values with increasing crack length, a feature that was seen for virtually all of the DCB tests performed with the stiffened facesheets. Interestingly, this was also seen in the high-temperature testing study that used stiffened facesheets.[11]

As mentioned in the section 3, energy methods can also be used. For specimen DCB11–11–05F the data to be used are shown in figure 20. The points are those labeled in figure 17 with a polynomial curve fit and extraneous points removed for clarity. The total area of surface formed on the specimen due to peeling was 9.04 in^2.

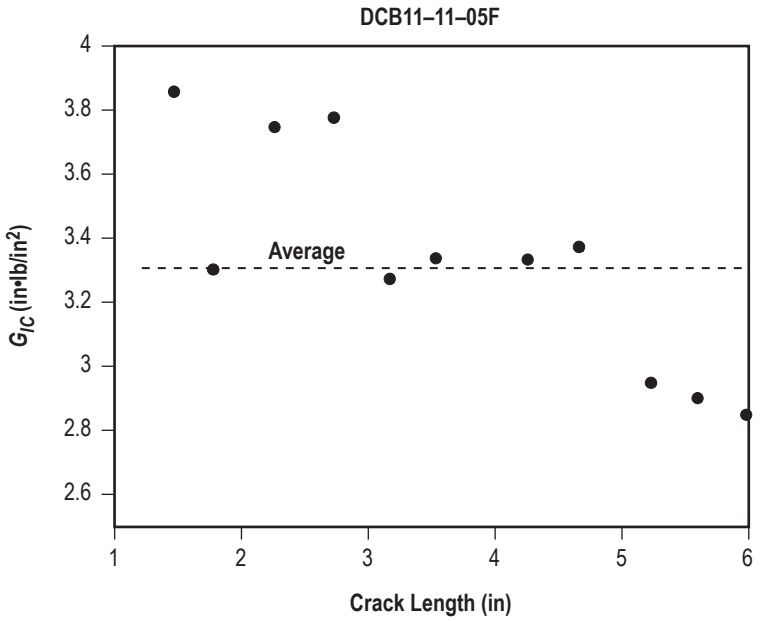

Figure 19. R-curve for data from specimen DCB11–11–05F.

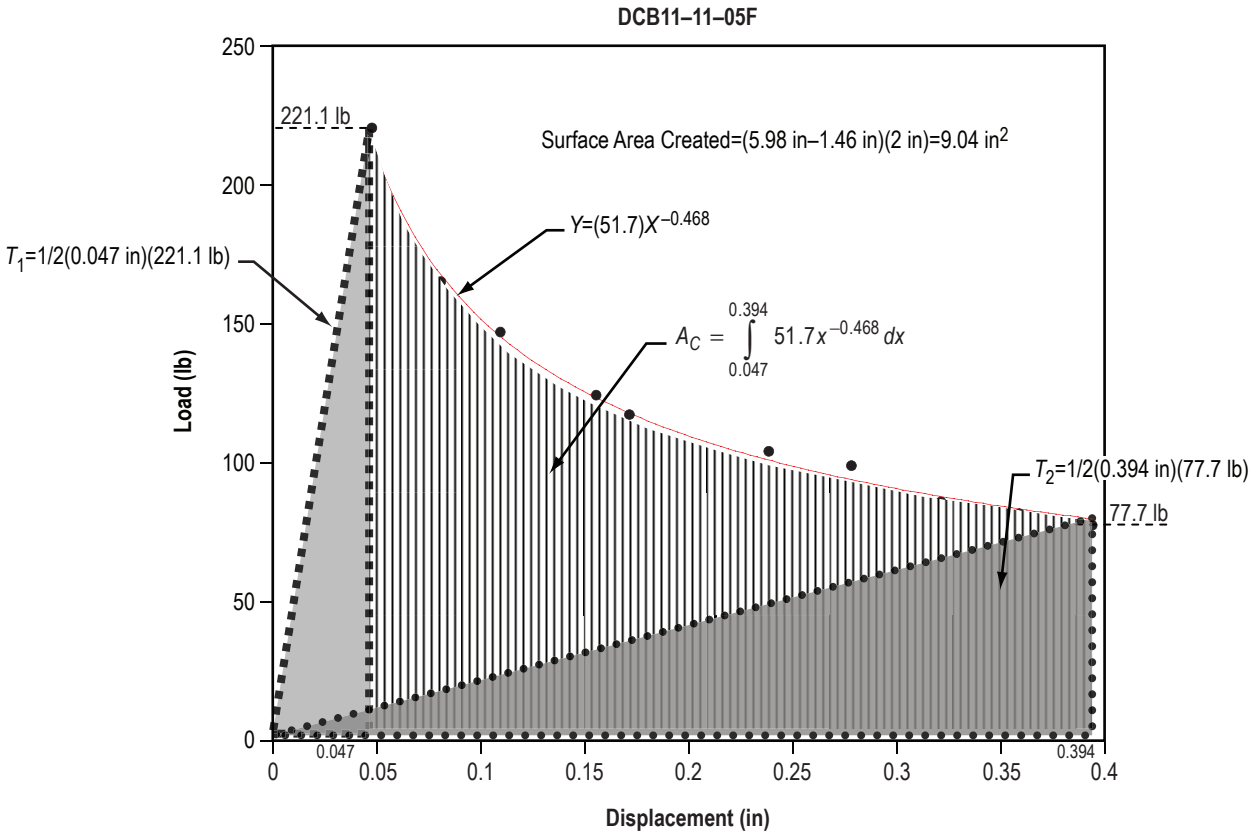

Figure 20. Data used to find G_{IC} on specimen DCB11–11–06E using energy methods.

The area under the curve, denoted by A_C, is given by evaluating the integral shown in the figure. In figure 20, triangle 1 (T_1) is shown with borders of square dots and triangle 2 (T_2) is shown with borders of round dots. To find the total energy put into peeling during this segment of growth, triangle 1 must be added and triangle 2 subtracted from the evaluated integral. For specimen DCB11–11–06E this turns out to be

$$E_T = \int_{0.047}^{0.394} 51.7x^{-0.468} + \frac{1}{2}(0.047)(221.1) - \frac{1}{2}(0.394)(77.7) =$$

$$\frac{51.7}{0.532} x^{0.532}\Big|_{0.047}^{0.394} + 5.2 - 15.3 = 30.1 \ \text{in} \cdot \text{lb} \ , \tag{17}$$

where E_T is the energy associated with peeling to create the area of 9.04 in^2. Thus, the G_{IC} value is 30.1 in·lb/9.04 in^2 = 3.3 in·lb/in^2.

Table 2 summarizes the data for all of the stiffened DCB tests performed. The plots used to generate these data are given in appendix B. The R-curves for these specimens are given in appendix C.

Table 2. Results of the stiffened DCB tests.

Specimen ID	Facing Thickness (Plies)	Pull Direction	G_{IC}(in•lb/in^2)	
			CC	Areas
DCB7–26–05–A	2	L	2.9	4.1
DCB7–26–05–B	2	L	3.7	4.5
DCB7–26–05–C	2	L	3	3
DCB7–26–05–D	2	L	2.9	2.8
DCB7–27–05–A	3	L	2.9	2.9
DCB7–27–05–B	3	L	2.9	2.8
DCB7–28–05–A	4	L	3.6	3.5
DCB7–28–05–B	4	L	3.8	3.5
DCB7–28–05–1A	2	W	3.4	3.5
DCB7–28–05–1B	2	W	4.7	4.8
DCB7–29–05–1A	3	W	4.5	4.5
DCB7–29–05–1B	3	W	4.7	4.5
DCB7–29–05–2A	4	W	3.3	3.3
DCB7–29–05–2B	4	W	3.2	3.4
DCB11–11–05E	2	L	3.3	3.3
DCB11–11–05F	2	L	3.3	3.3
DCB11–11–05G	2	L	3.1	3.5
DCB11–11–05H	2	L	3.4	3.6
		Average	3.5	3.6

5.2.2 Specimens Without Stiffening Plates

For the second series of tests, stiffeners were not bonded to the specimens and loaded as shown in the experimental section. A typical load-displacement curve from this type of test is shown in figure 21.

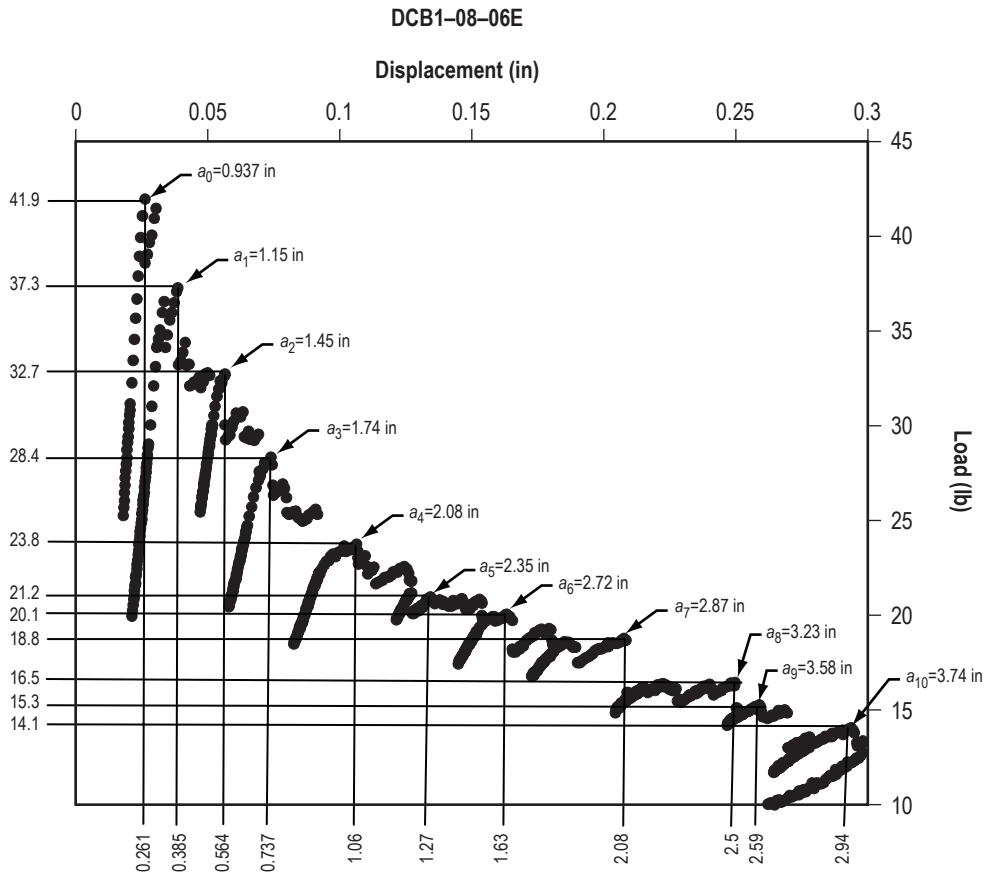

Figure 21. Typical load-displacement data from the second series of DCB nonstiffened tests.

The data used to determine the critical strain energy release rate are plotted in figure 21. Equations (2) and (3) were used to find the critical strain energy release rate. A compliance versus crack length plot is made first and a power law is made to fit to it. This is shown in figure 22 for the data of specimen DCB1–08–06E. The power-law fit gives constants of C_0=0.007 (in/lb·in^n) and n=2.55 for equation (2). Equation (3) will become

$$G_{IC} = \frac{P^2}{2(2\text{in})} 2.55 \left(0.007 \frac{\text{in}}{\text{lb} \cdot \text{in}^{2.55}} \right) a^{1.55} \quad . \tag{19}$$

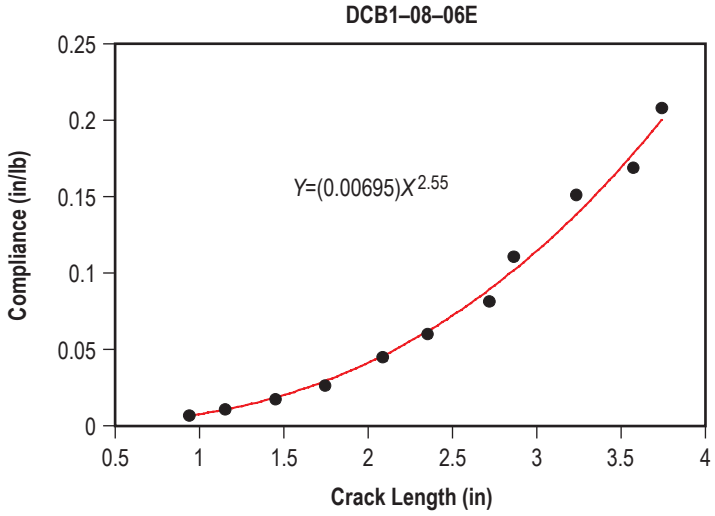

Figure 22. Compliance versus crack length with a power-law fit.

Using the values in figure 21 for the measured loads and associated crack lengths gives an average G_{IC} value of 7.7 in·lb/in^2 for all 11 data points. The R-curve for the data is shown in figure 23. These data display no discreet trend in G_{IC} value with increasing crack length.

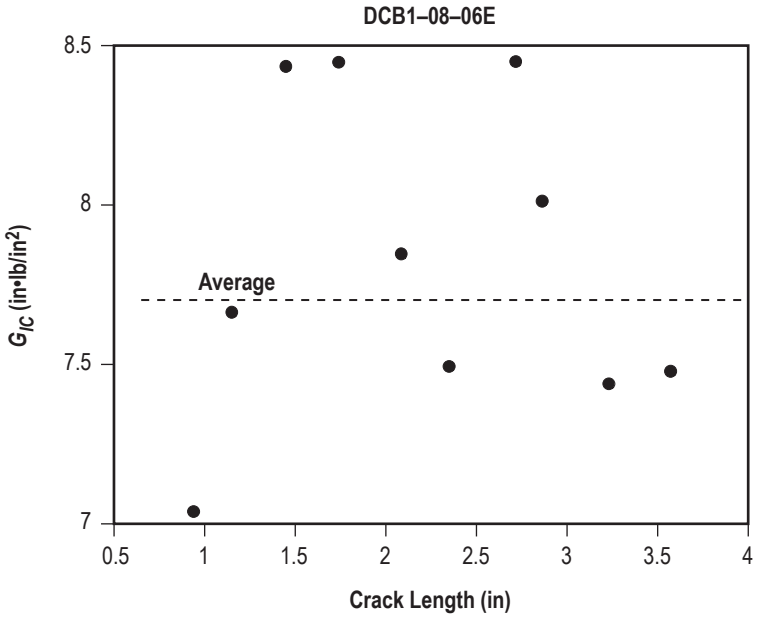

Figure 23. R-curve for data from specimen DCB1–08–06E.

Unlike the stiffened specimens, the facesheet thickness on these specimens would have more of an influence on the test. For this reason, a variety of facesheet thicknesses were tested. For specimens with facesheets only 1- or 2-plies thick, the facesheet being peeled would break off before any meaningful measurements could be made. A picture of this early facesheet breakage is shown in figure 24.

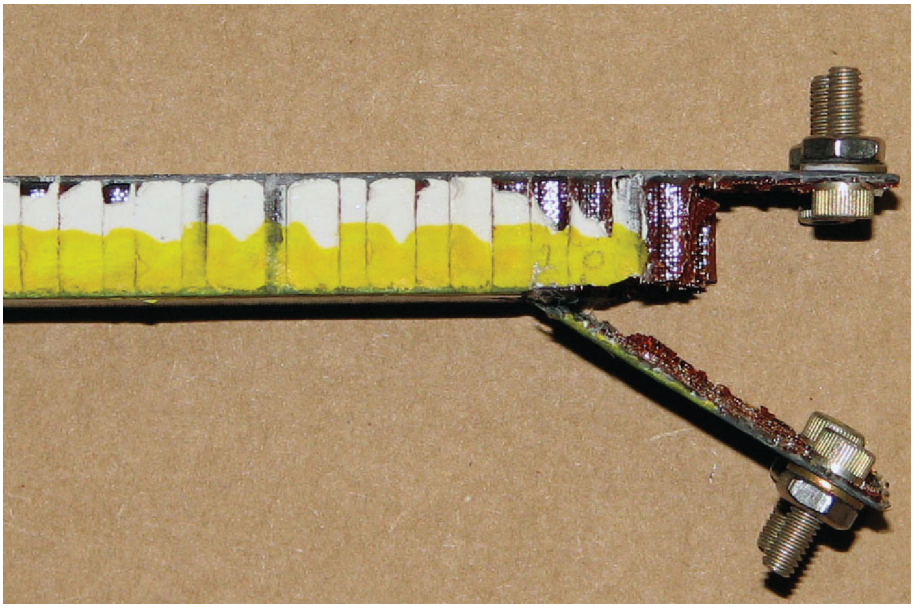

Figure 24. DCB specimen with 2-ply facesheets showing early facesheet breakage.

It was found that three plies of facesheet would provide data before the facesheet broke and that the facesheets never broke on specimens with four or more plies. A summary of the nonstiffened specimen results is presented in table 3. The plots used to generate these data are given in appendix D. The R-curves for these specimens are given in appendix E.

Table 3. Results of the nonstiffened DCB tests.

Specimen ID	Facing Thickness (Plies)	Pull Direction	G_{IC} (in•lb/in^2)	
			CC	Areas
DCB11–09–05A	3	L	6.3	7
DCB11–09–05B	3	L	6.5	6.9
DCB11–09–05C	3	L	6.6	7.9
DCB11–09–05E	3	L	7.7	7.6
DCB11–21–05A	4	L	7.5	7.7
DCB11–21–05B	4	L	6.2	6.8
DCB11–21–05C	4	L	6.9	7.1
DCB2–17–06A	4 (4 p.c.f. core)	L	6.9	6.8
DCB2–17–06B	4 (4 p.c.f. core)	L	6.4	6.2
DCB1–08–06A	5	L	7	7.1
DCB1–08–06B	5	L	8.1	7.7
DCB1–08–06C	5	L	8	7.9
DCB1–08–06E	5	L	7.7	7.8
DCB1–08–06F	5	L	8.3	7.8
DCB1–20–06A	8	L	7.1	7.8
DCB1–20–06B	8	L	8.9	9.2
DCB1–20–06C	8	L	8.1	8.4
DCB1–20–06D	8	L	7.4	7.3
DCB1–20–06E	8	L	7	7.3
		Average	7.7	7.5

5.2.3 Comparison of the Two Different Double Cantilever Beam Tests

The two types of DCB specimens that have been used are referred to as stiff and nonstiffened, which essentially describes the flexibility of the facings. For both types of specimens, a disbond of the facesheet to the core was initiated and allowed to grow naturally before measurements were taken. The disbond was grown and the load and displacement data were taken as called for in ASTM D5528, but with minor modifications since the disbond displayed extreme stick-slip behavior.

The first major difference in these two test specimens was that the relatively lightweight core (4 lb/ft^3) stiff specimen failed in the center of the core, as shown in figure 25.

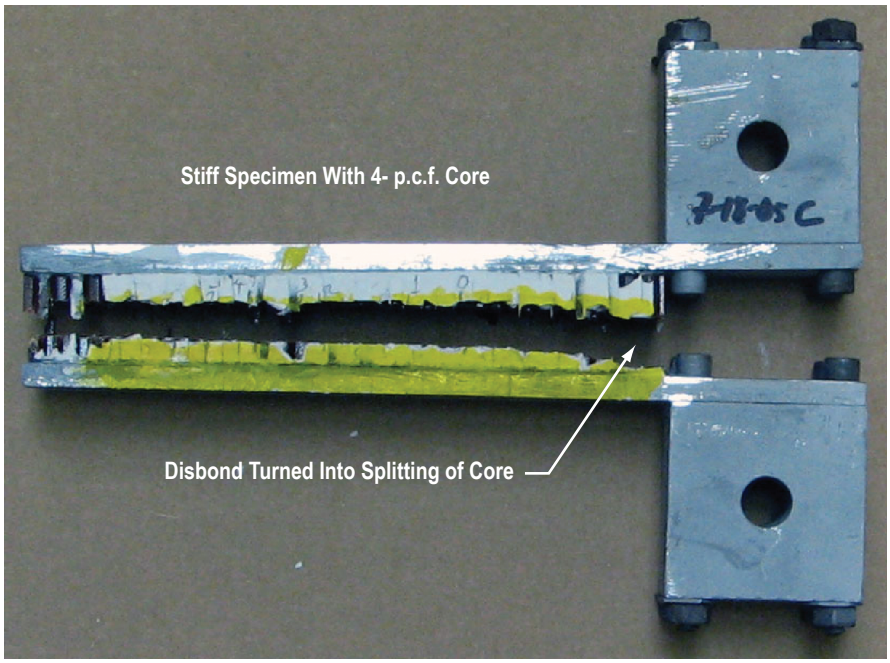

Figure 25. Stiff DCB specimen showing splitting of the 4-lb/ft^3 core.

The nonstiffened 4-lb/ft^3 core specimens disbonded at the core/facesheet interface. When the core density was raised to 8 lb/ft^3, both types of specimens failed at the core/facesheet bond. At this point it is interesting to note that the 4-lb/ft^3 core FWT specimens failed in the core (as it should) and 8-lb/ft^3 core failed at the core/facesheet bond.

As the specimens with the 8-lb/ft^3 core were tested, other differences became apparent as follows:

- The stiff specimens took a much higher load and much smaller displacement to grow the disbond.
- The G_{IC} calculated for the stiff specimens was consistently about one half or less of the nonstiffened specimens.

- The G_{IC} values for the nonstiffened specimens were similar to that calculated by the CD peel test.
- The stiff specimens R-curve data usually showed a rapid G_{IC} drop with increasing crack length.
- The R-curve data for the nonstiffened specimens showed a fairly consistent value for G_{IC} after the first measurement, which was usually low.
- The nonstiffened specimens had rather large deflections (approaching the crack length in some cases). Large deflections for a DCB test have been examined in another study and will be briefly mentioned in this TP.[16]
- The fracture surfaces of the two specimens looked different, especially the honeycomb.
- The stiff specimen fracture surface looked like an FWT specimen, while the nonstiffened specimen fracture surface looked like a CDP specimen.

Figure 26 shows the fracture surfaces of the stiff, nonstiffened, FWT, and CD specimens.

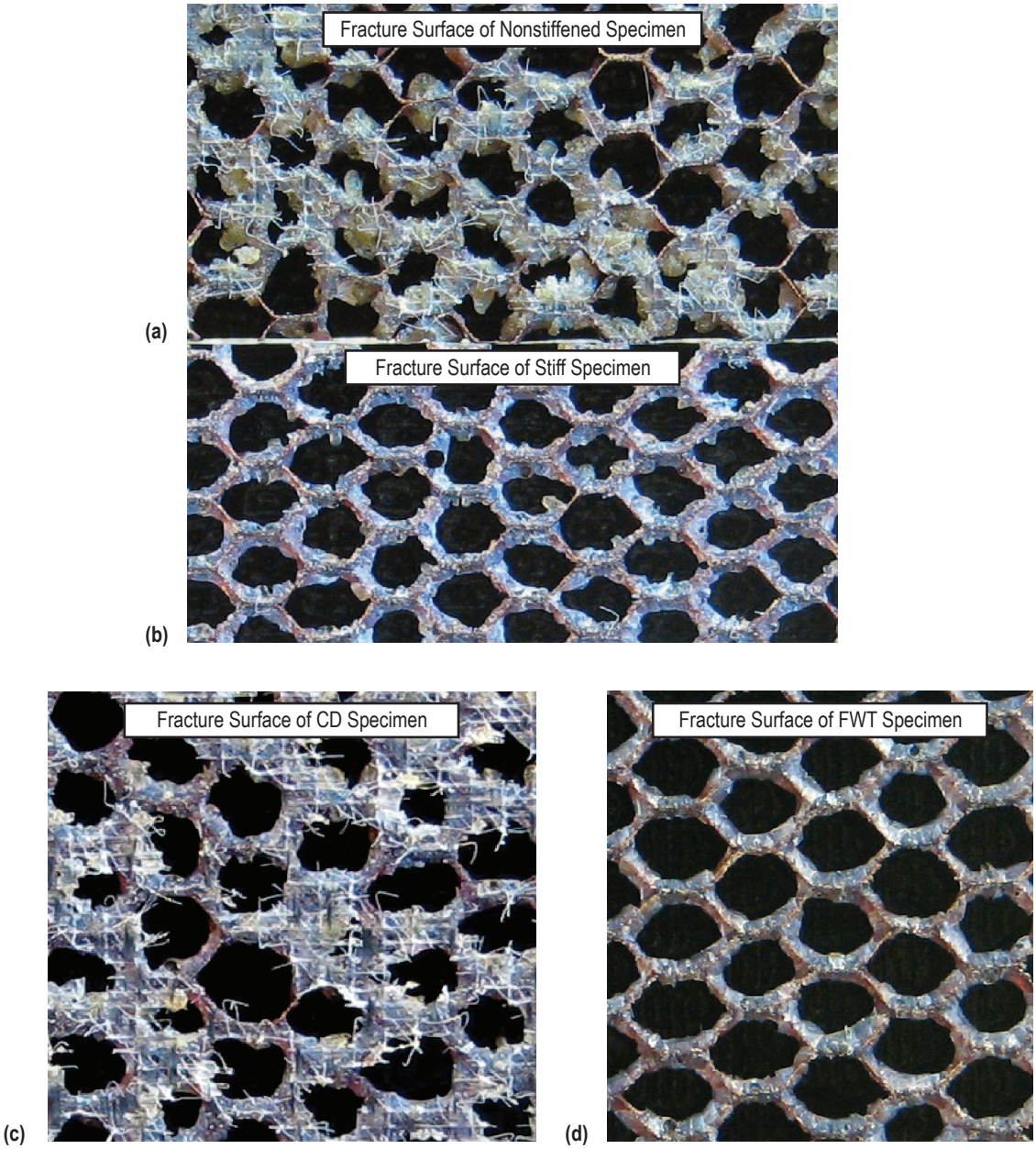

Figure 26. Photographs of the fracture surfaces of the (a) nonstiffened, (b) stiff, (c) CD, and (d) FWT specimens.

It appears that the stiff specimens are behaving more like a FWT test than a true peel test. This is quite plausible for a facing being peeled from a rather compliant surface (the honeycomb). The following schematic describes the mechanics behind the problem.

For the stiff specimens, the crack is propagated more by the tensile stresses in the core acting over a relatively large area, as shown in figure 27.

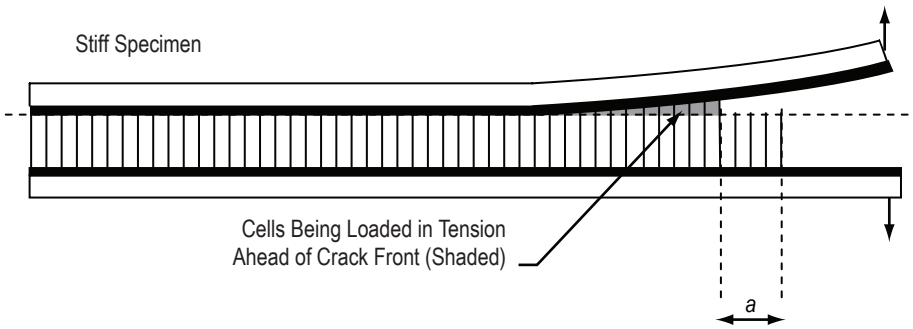

Figure 27. Schematic of stiffened specimen during testing.

The geometry of the nonstiffened specimen approaches that of a T-peel test with the forces concentrated entirely at the crack front, as shown in figure 28.

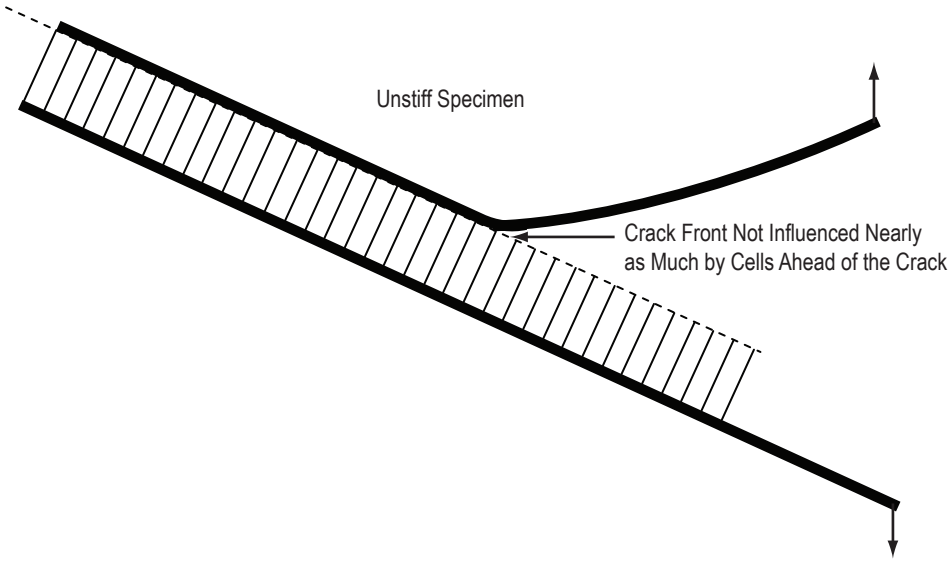

Figure 28. Schematic of nonstiffened specimen during testing.

The nonstiffened specimens underwent large deflections, the main affect which is the effective shortening of the moment arm. This was examined in detail for laminate DCB testing in reference 16. Results from this study are shown in nondimensional form in figure 29.

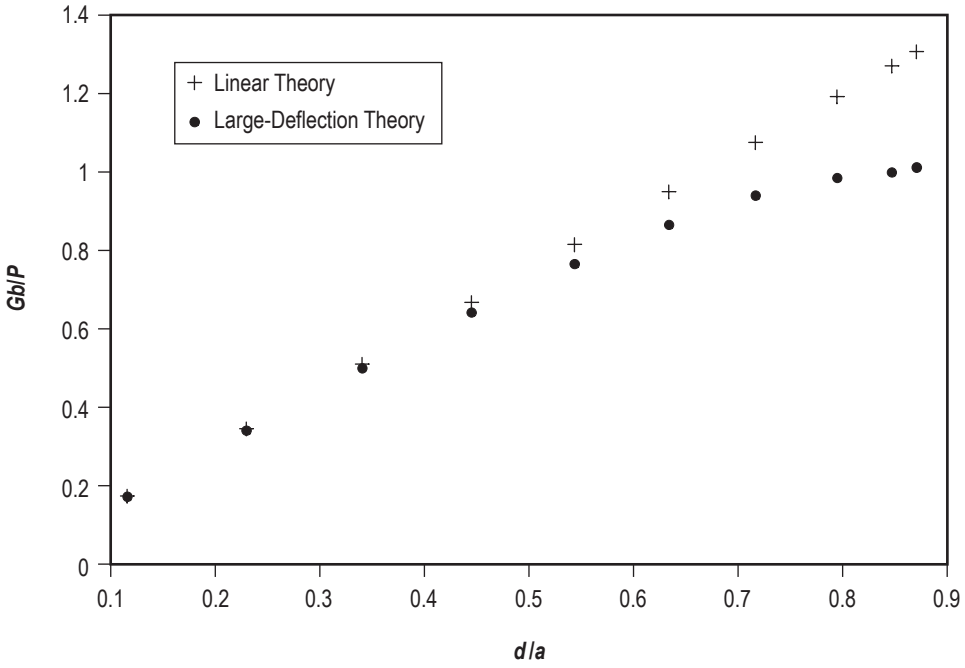

Figure 29. Nondimensional strain energy release rate for a cantilevered beam, from reference 16.

Figure 29 shows that the strain energy release rate does not vary much from the linear beam theory until d/a reaches about 0.6. This amount of deflection occurred in all specimens except those that had 8-ply facesheets. The deviations are on the order of 30-percent magnitude at the largest deflections, however the scatter within G_{IC} values on the R-curves varied more than this for many of the specimens, so a detailed analysis including large-deflection theory would be of little practical use in this study.

Interestingly, the same results for G_{IC} are obtained whether energy methods (area under load-displacement curve divided by surface area created) or the CC method is used. A study using stiffeners on a composite laminate (not sandwich) specimen, determined that no correction factors are needed when reducing DCB test data.[17]

6. CONCLUSIONS

From the data presented, it appears that artificially stiffening DCB specimens cause the tests to behave more like an FWT test than a peel test. This was evidenced by the splitting of the 4-lb/ft^3 core, the fracture surface appearance, and the unusually low G_{IC} values. The nonstiffened specimens, even the 8-ply thick facesheets, were much more compliant (about 30-times less bending stiffness) than the 0.25-in thick aluminum plates. It would be interesting to continue the tests using more plies of facesheet to see if a transition region exists where the failure mode begins to change from peel to tensile. The data presented in this TP clearly indicates that the nonstiffened specimens failed in peel. The average critical strain energy release rate was 7.3 in·lb/in^2 using the CC data reduction technique, and 7.5 in·lb/in^2 using the areas reduction technique, which compared well with the 7.5 in·lb/in^2 CD peel method result.

Using the areas method to reduce the data was needed in this study since the nonstiffened specimens underwent very large deflections. The areas method also is independent of specimen geometry and gave results similar to those calculated by the CC method despite the large deflections.

Critical strain energy release rates from the CD peel tests tended to be slightly more consistent with a standard deviation of 5.7 percent of the mean (n=29), while the DCB tests gave a standard deviation of 10.4 percent (CC) and 8.9 percent (areas) of the mean (n=19).

Overall, from the data presented here, it appears that the CD peel and DCB tests without facesheet stiffeners are valid methods of determining G_{IC} of a core/facesheet bond.

APPENDIX A—DATA FROM THE CLIMBING DRUM PEEL TESTS

Plots used for CD peel test results, along with the load to roll up the facesheet and the load to peel.

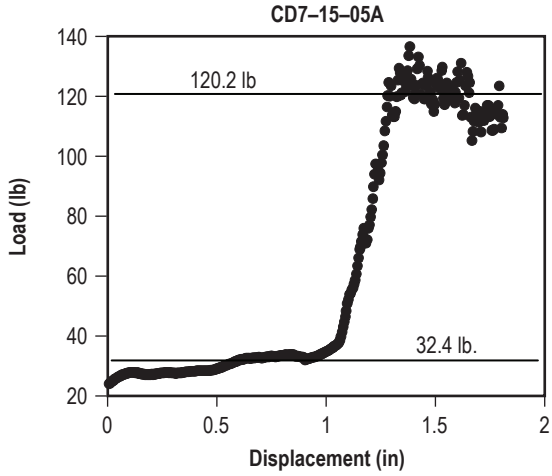

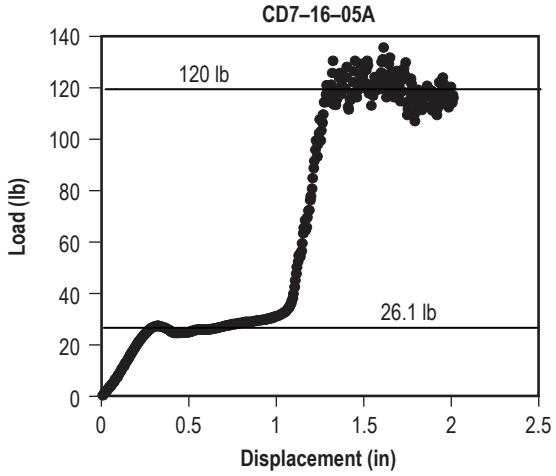

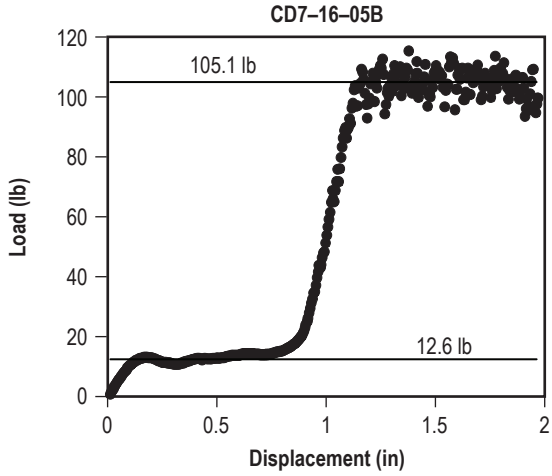

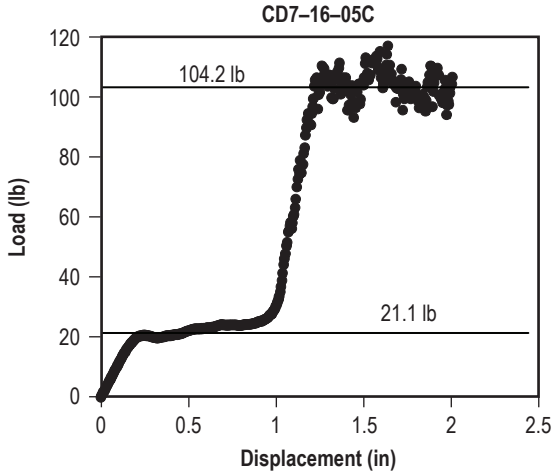

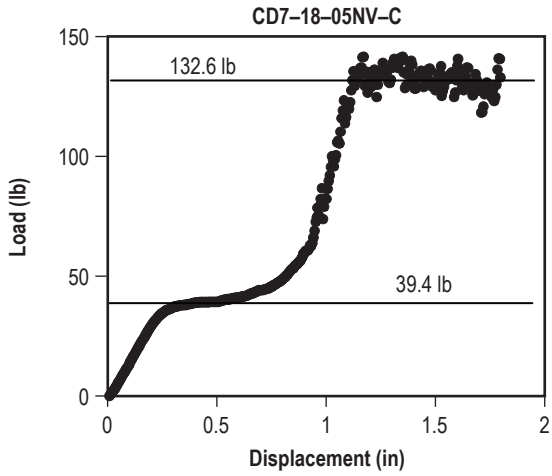

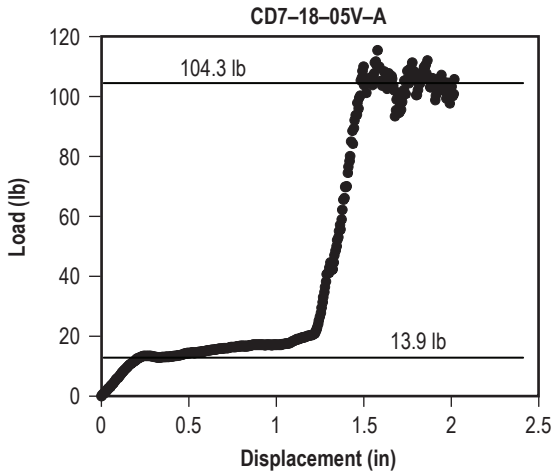

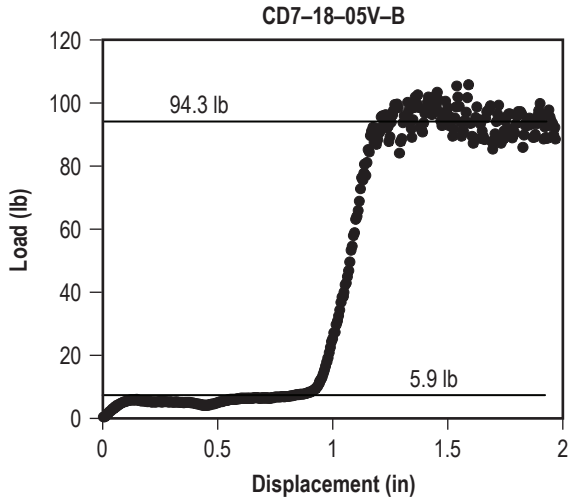
CD7–18–05V–B
94.3 lb
5.9 lb
Load (lb)
Displacement (in)

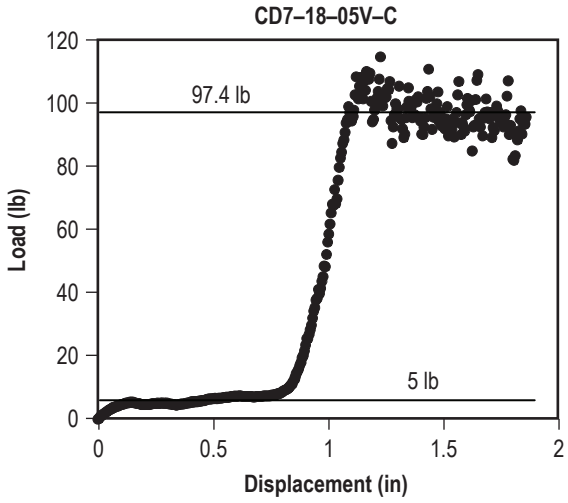
CD7–18–05V–C
97.4 lb
5 lb
Load (lb)
Displacement (in)

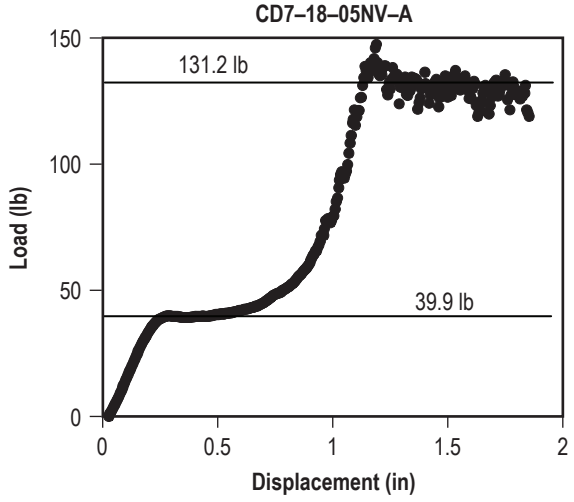
CD7–18–05NV–A
131.2 lb
39.9 lb
Load (lb)
Displacement (in)

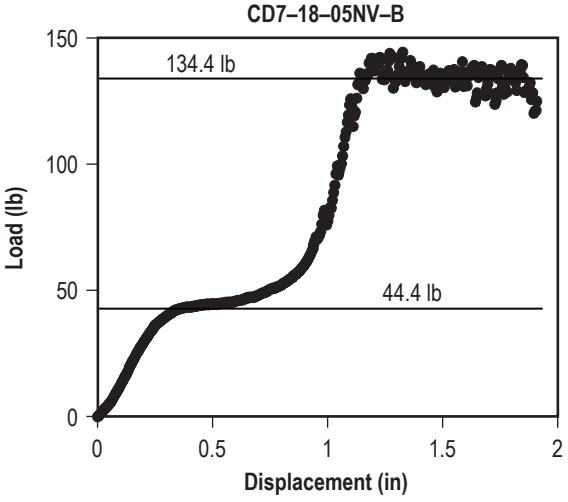
CD7–18–05NV–B
134.4 lb
44.4 lb
Load (lb)
Displacement (in)

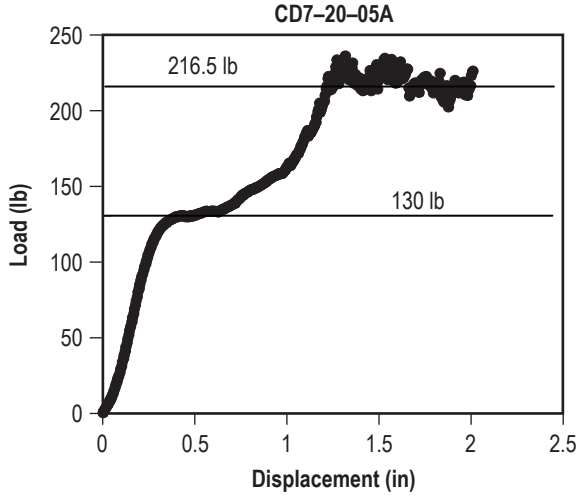
CD7–20–05A
216.5 lb
130 lb
Load (lb)
Displacement (in)

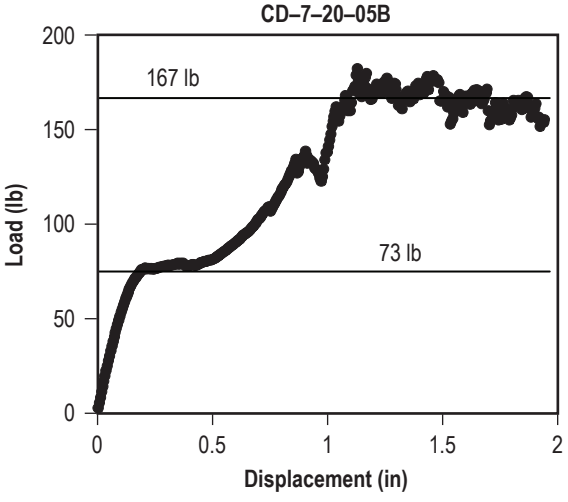
CD–7–20–05B
167 lb
73 lb
Load (lb)
Displacement (in)

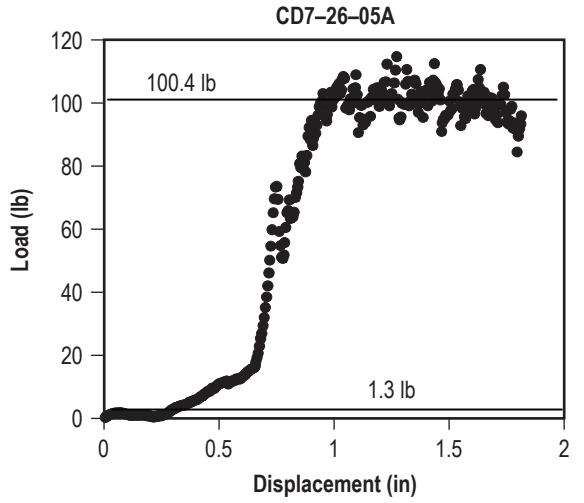
CD7–26–05A
100.4 lb
1.3 lb
Load (lb)
Displacement (in)

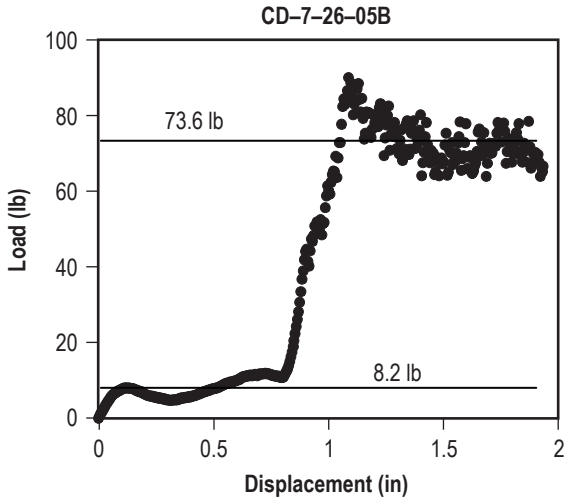
CD–7–26–05B
73.6 lb
8.2 lb
Load (lb)
Displacement (in)

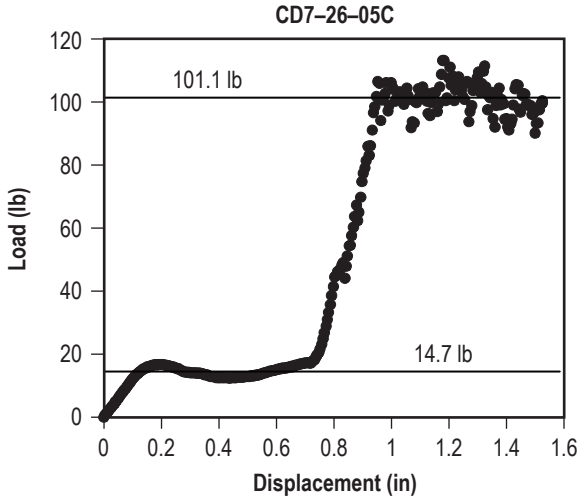
CD7–26–05C
101.1 lb
14.7 lb
Load (lb)
Displacement (in)

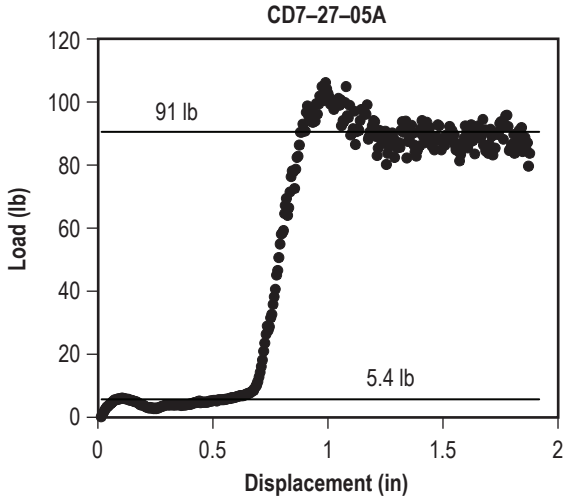
CD7–27–05A
91 lb
5.4 lb
Load (lb)
Displacement (in)

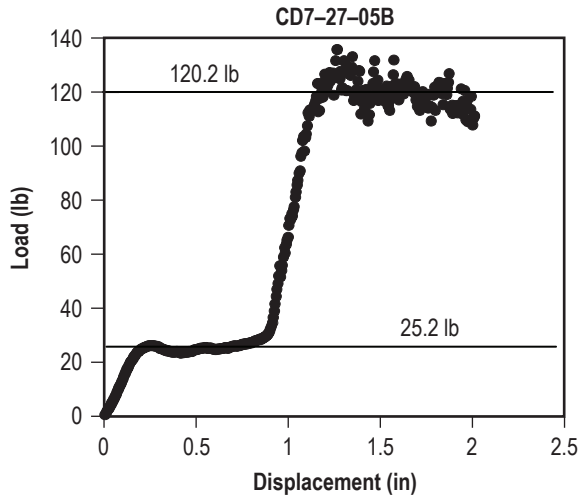
CD7–27–05B
120.2 lb
25.2 lb
Load (lb)
Displacement (in)

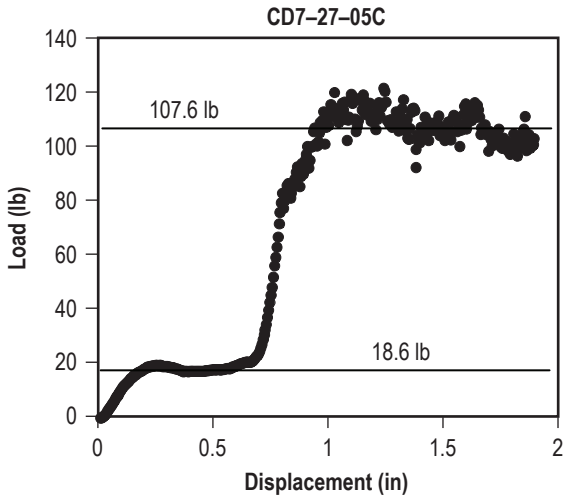
CD7–27–05C
107.6 lb
18.6 lb
Load (lb)
Displacement (in)

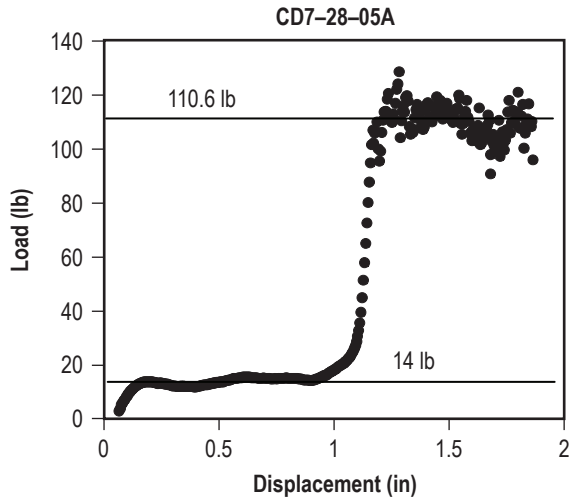
CD7–28–05A
110.6 lb
14 lb
Load (lb)
Displacement (in)

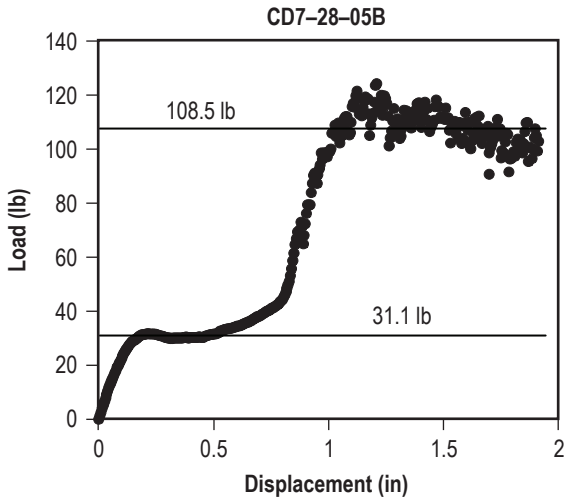
CD7–28–05B
108.5 lb
31.1 lb
Load (lb)
Displacement (in)

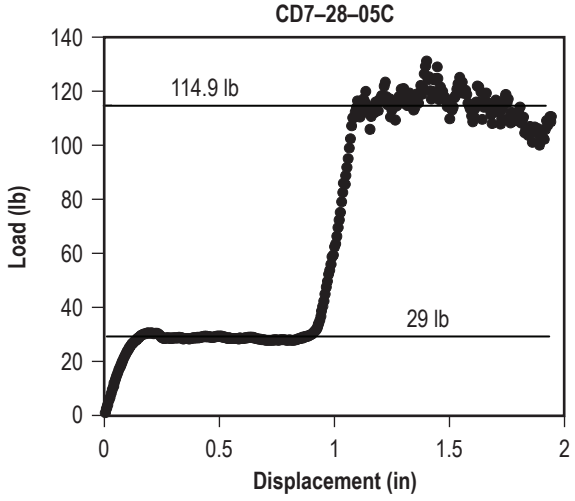
CD7–28–05C
114.9 lb
29 lb
Load (lb)
Displacement (in)

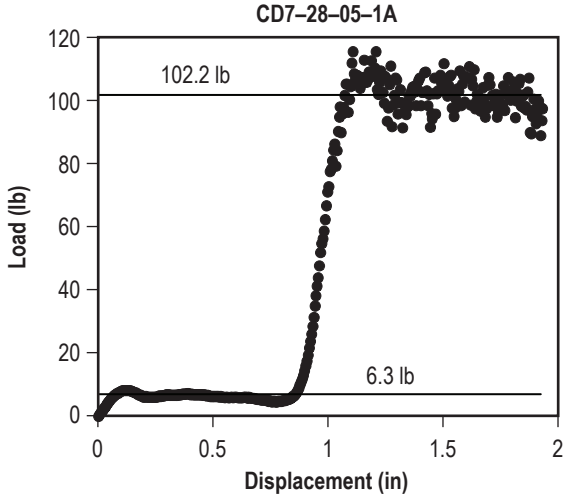
CD7–28–05–1A
102.2 lb
6.3 lb
Load (lb)
Displacement (in)

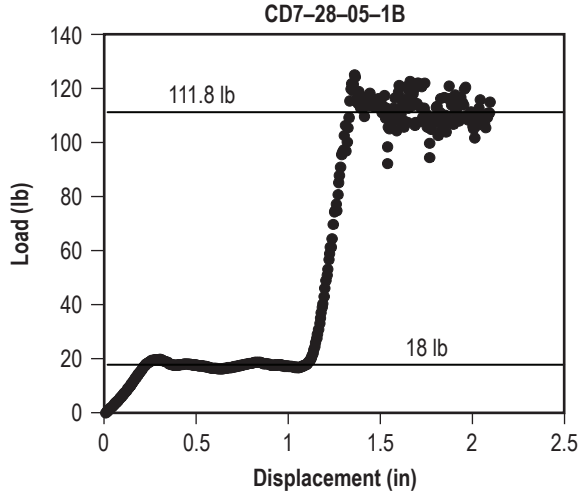
CD7–28–05–1B
111.8 lb
18 lb
Load (lb)
Displacement (in)

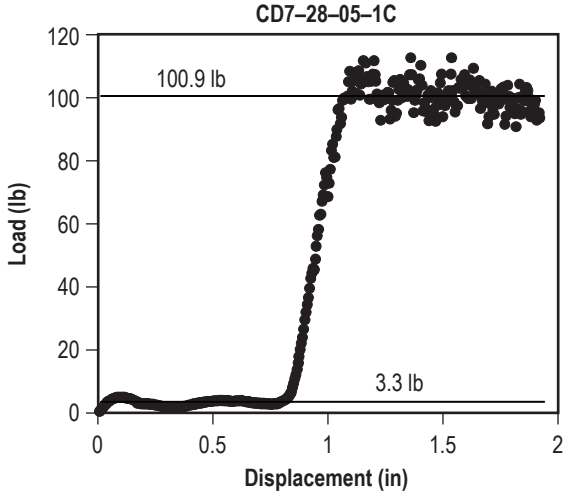
CD7–28–05–1C
100.9 lb
3.3 lb
Load (lb)
Displacement (in)

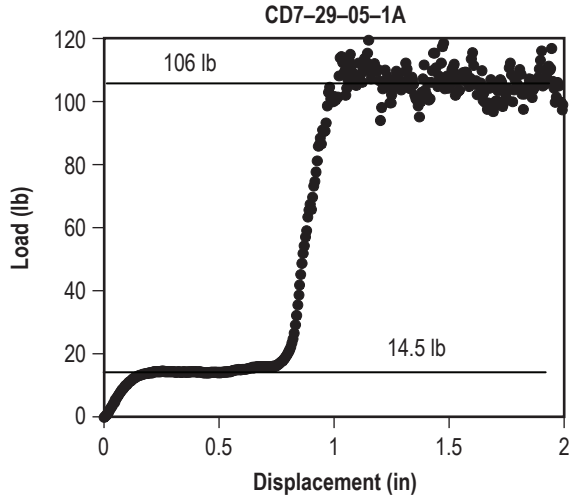
CD7–29–05–1A
106 lb
14.5 lb
Load (lb)
Displacement (in)

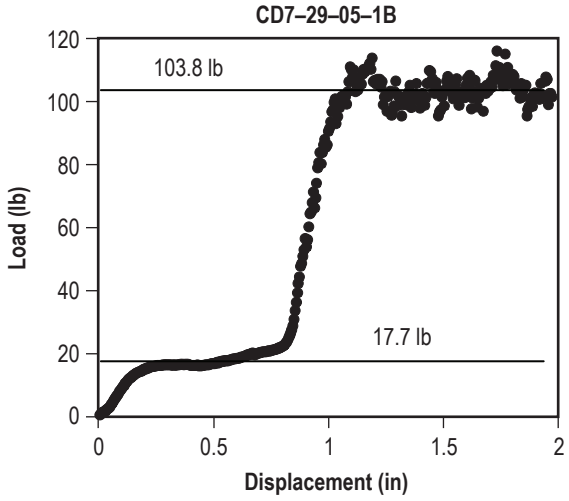
CD7–29–05–1B
103.8 lb
17.7 lb
Load (lb)
Displacement (in)

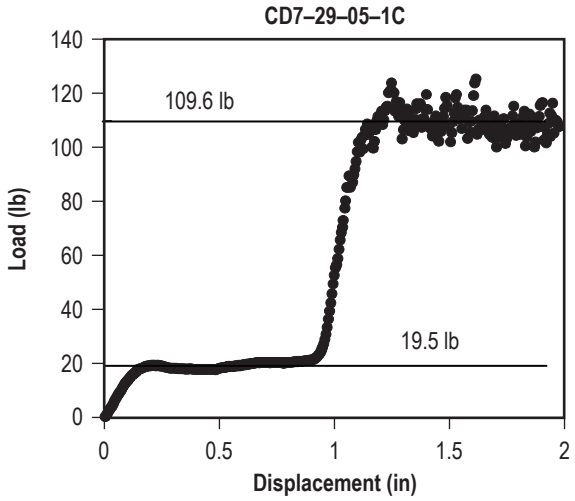
CD7–29–05–1C
109.6 lb
19.5 lb
Load (lb)
Displacement (in)

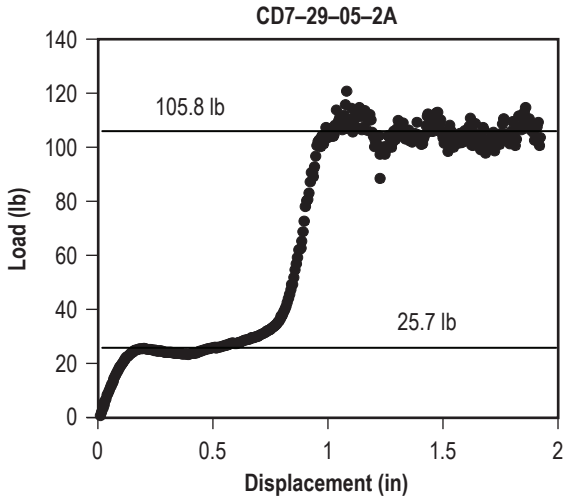
CD7–29–05–2A
105.8 lb
25.7 lb
Load (lb)
Displacement (in)

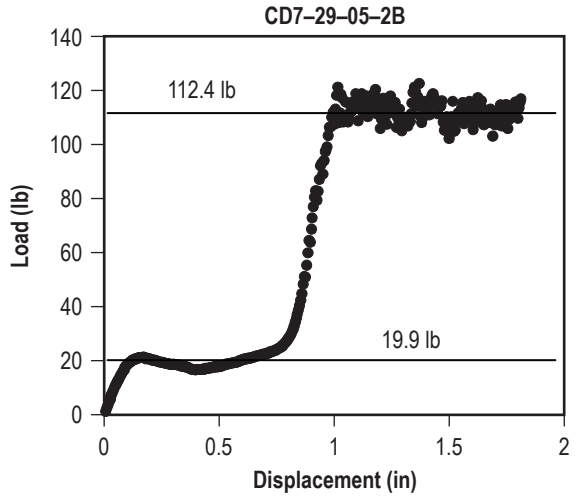
CD7–29–05–2B
112.4 lb
19.9 lb
Load (lb)
Displacement (in)

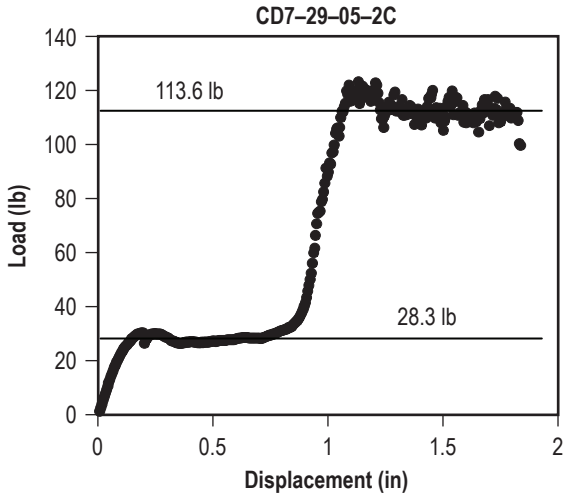
CD7–29–05–2C
113.6 lb
28.3 lb
Load (lb)
Displacement (in)

APPENDIX B—DATA FROM THE DOUBLE CANTILEVER BEAM TESTS WITH STIFFENERS

Plots used to generate the stiffened DCB test data.

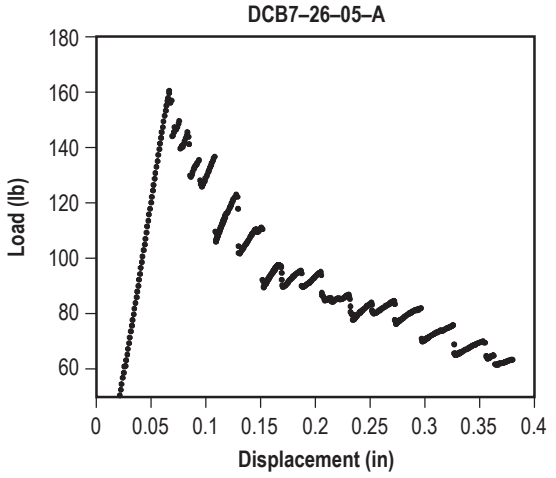

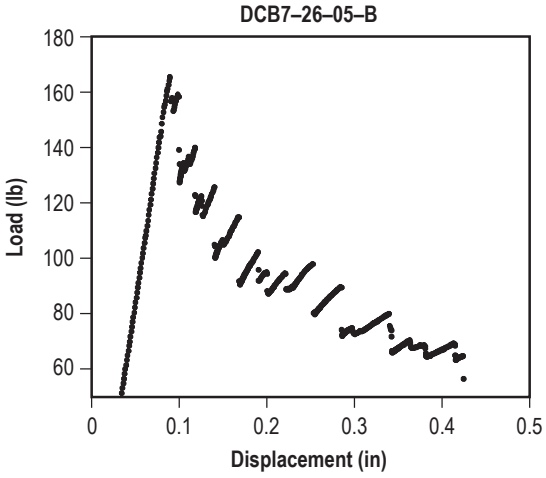

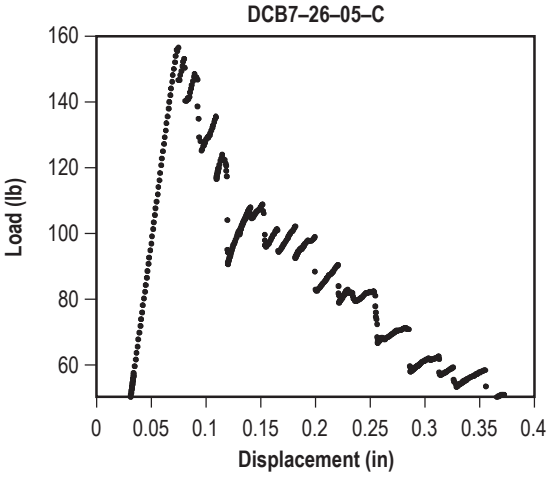

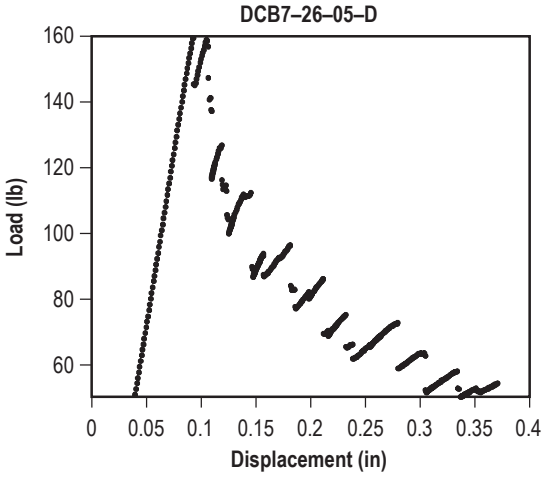

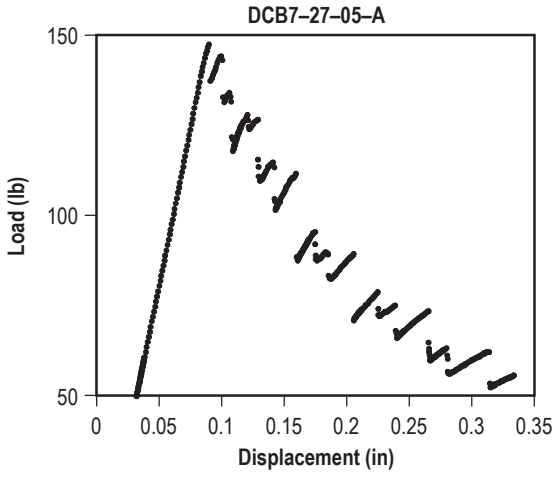

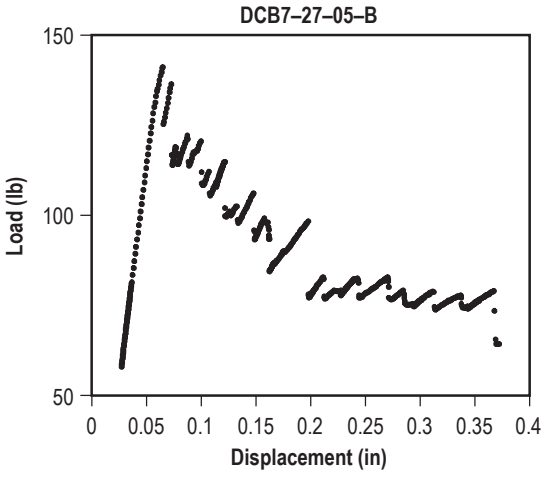

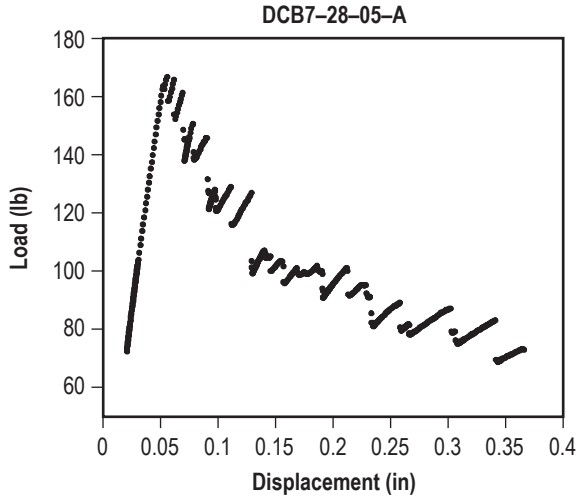
DCB7–28–05–A
Load (lb)
180
160
140
120
100
80
60
0
0.05
0.1
0.15
0.2
0.25
0.3
0.35
0.4
Displacement (in)

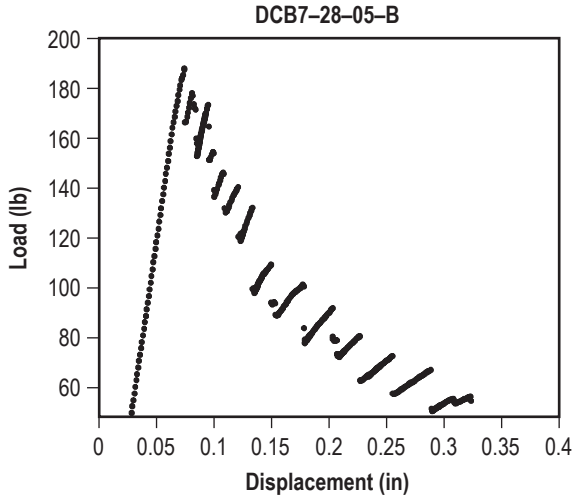
DCB7–28–05–B
Load (lb)
200
180
160
140
120
100
80
60
0
0.05
0.1
0.15
0.2
0.25
0.3
0.35
0.4
Displacement (in)

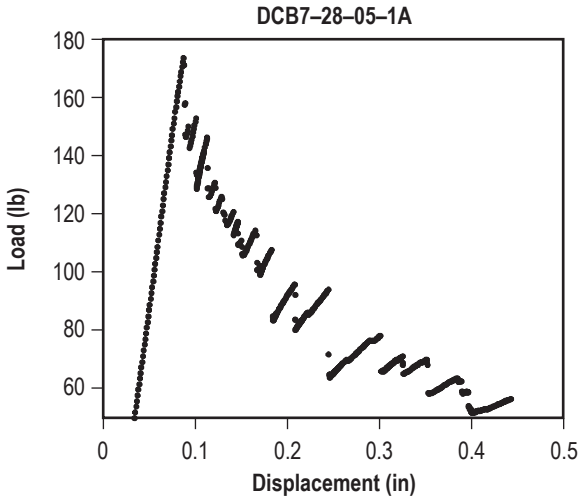
DCB7–28–05–1A
Load (lb)
180
160
140
120
100
80
60
0
0.1
0.2
0.3
0.4
0.5
Displacement (in)

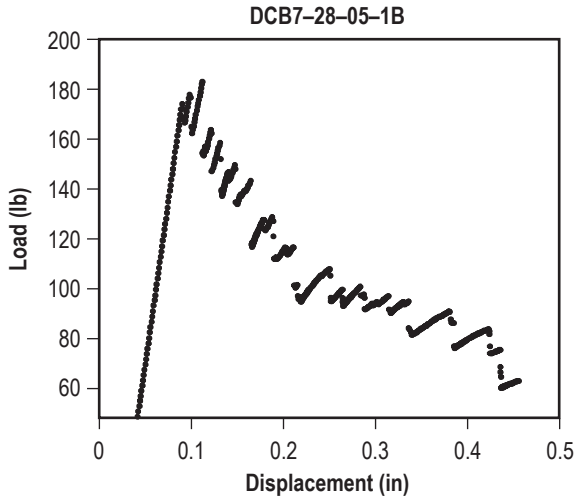
DCB7–28–05–1B
Load (lb)
200
180
160
140
120
100
80
60
0
0.1
0.2
0.3
0.4
0.5
Displacement (in)

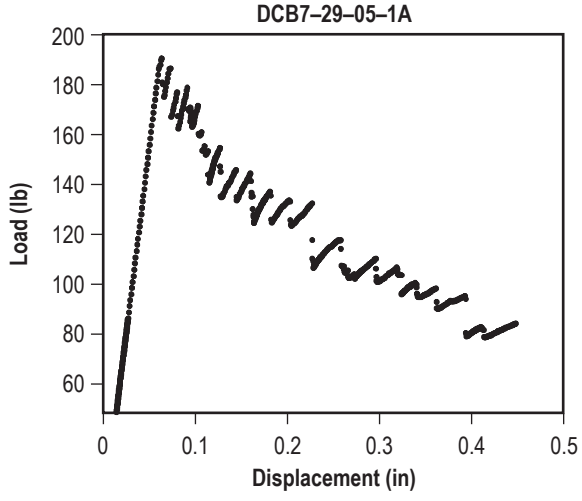
DCB7–29–05–1A
Load (lb)
200
180
160
140
120
100
80
60
0
0.1
0.2
0.3
0.4
0.5
Displacement (in)

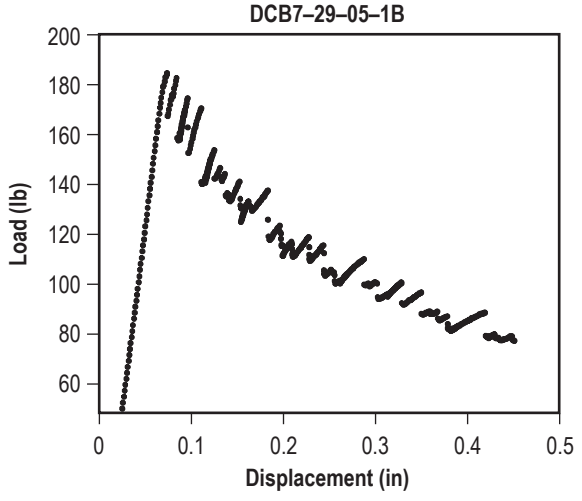
DCB7–29–05–1B
Load (lb)
200
180
160
140
120
100
80
60
0
0.1
0.2
0.3
0.4
0.5
Displacement (in)

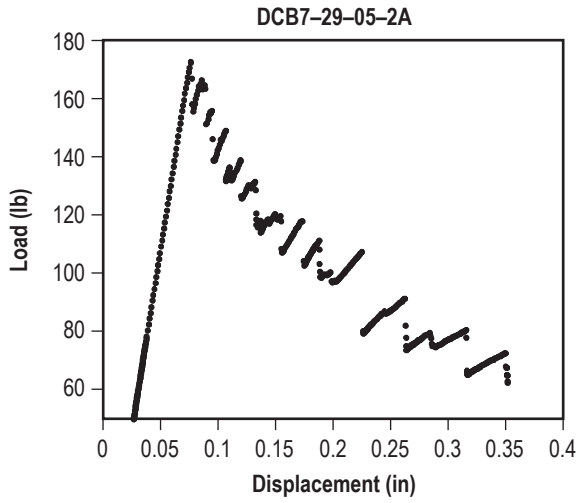
DCB7–29–05–2A
Load (lb)
180
160
140
120
100
80
60
0
0.05
0.1
0.15
0.2
0.25
0.3
0.35
0.4
Displacement (in)

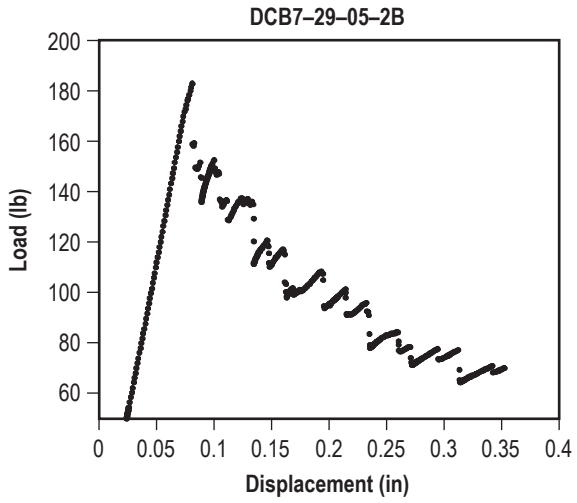
DCB7–29–05–2B
Load (lb)
200
180
160
140
120
100
80
60
0
0.05
0.1
0.15
0.2
0.25
0.3
0.35
0.4
Displacement (in)

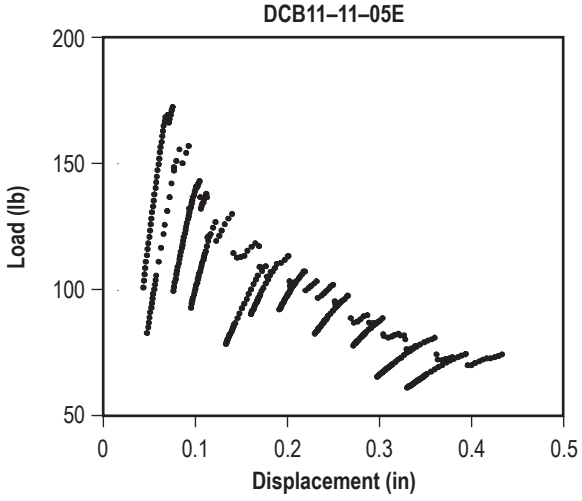
DCB11–11–05E
Load (lb)
200
150
100
50
0
0.1
0.2
0.3
0.4
0.5
Displacement (in)

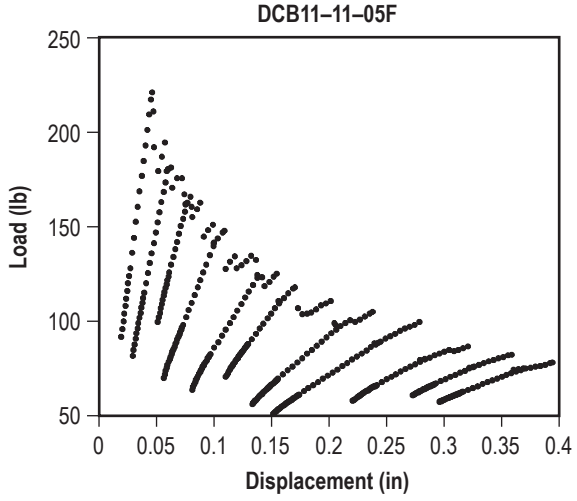
DCB11–11–05F
Load (lb)
250
200
150
100
50
0
0.05
0.1
0.15
0.2
0.25
0.3
0.35
0.4
Displacement (in)

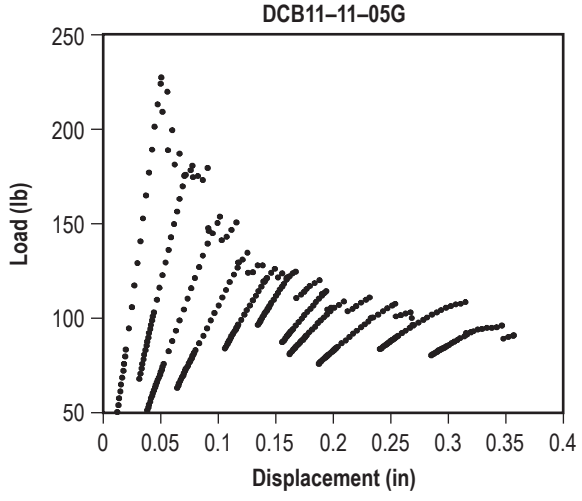
DCB11–11–05G
Load (lb)
250
200
150
100
50
0
0.05
0.1
0.15
0.2
0.25
0.3
0.35
0.4
Displacement (in)

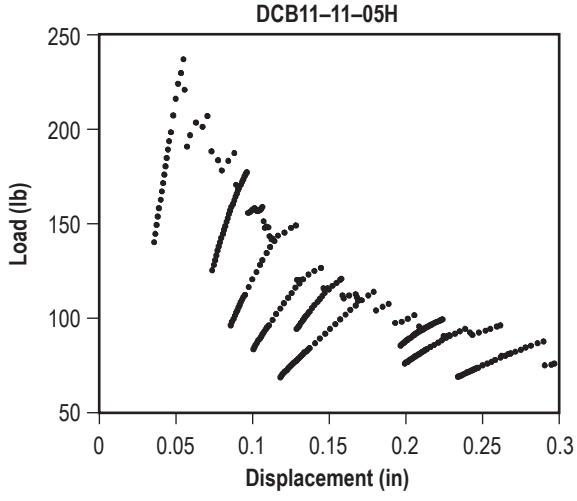
DCB11–11–05H
Load (lb)
250
200
150
100
50
0
0.05
0.1
0.15
0.2
0.25
0.3
Displacement (in)

APPENDIX C—R-CURVES FOR THE DOUBLE CANTILEVER BEAM TESTS WITH STIFFENERS

Plots used to generate R-curves of the stiffened DCB tests.

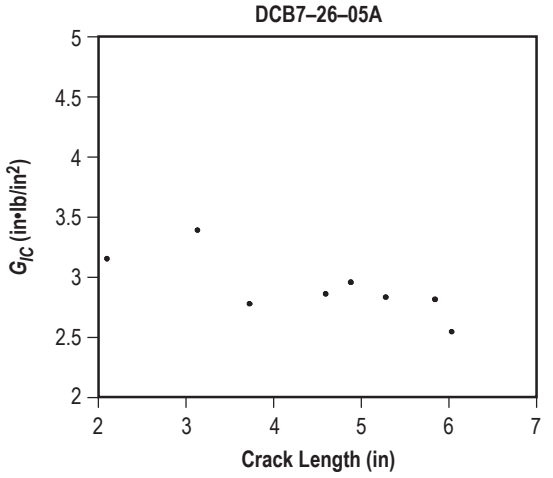

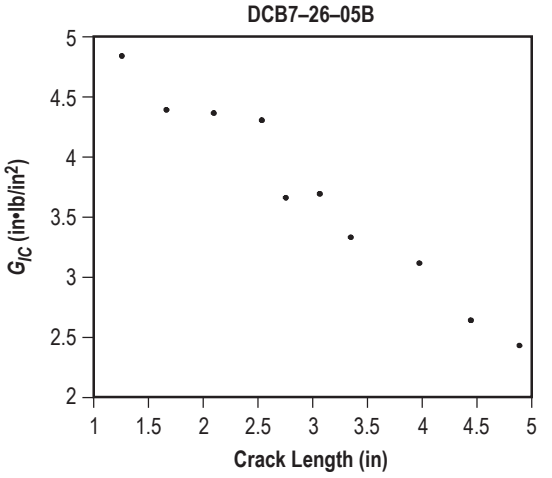

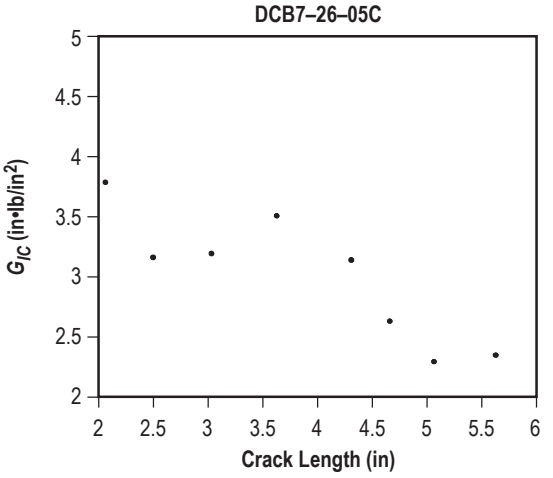

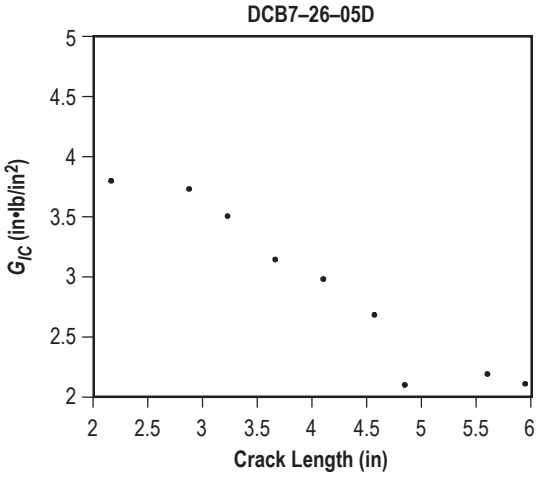

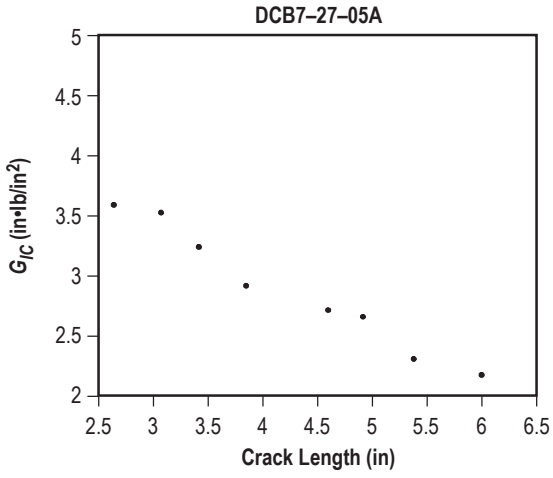

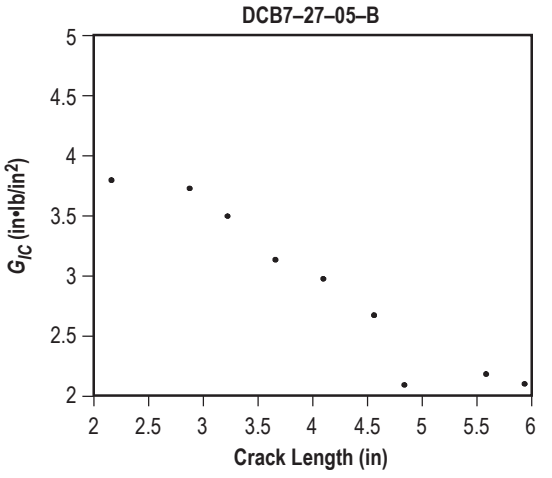

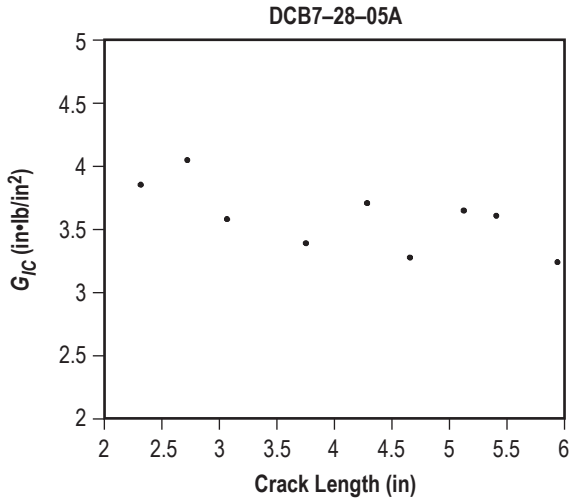
DCB7–28–05A
G_{IC} (in•lb/in^2)
Crack Length (in)

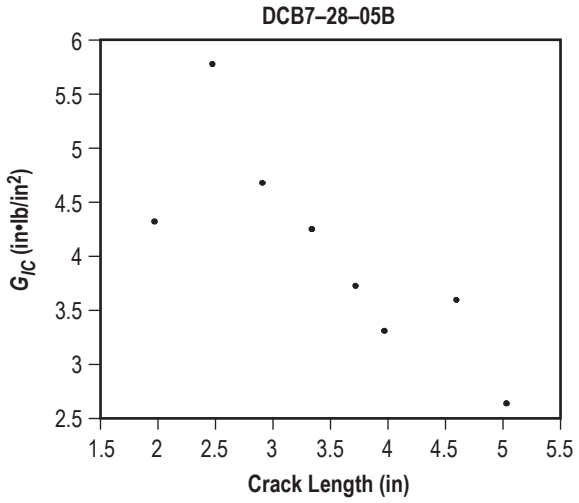
DCB7–28–05B
G_{IC} (in•lb/in^2)
Crack Length (in)

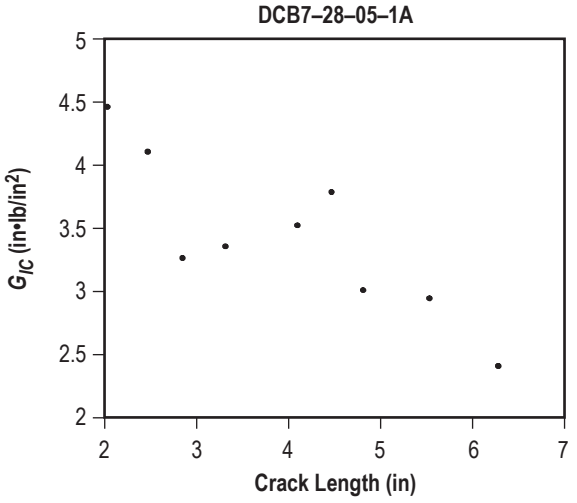
DCB7–28–05–1A
G_{IC} (in•lb/in^2)
Crack Length (in)

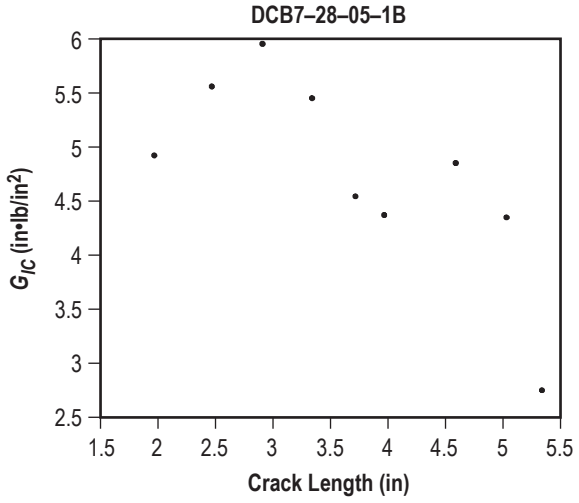
DCB7–28–05–1B
G_{IC} (in•lb/in^2)
Crack Length (in)

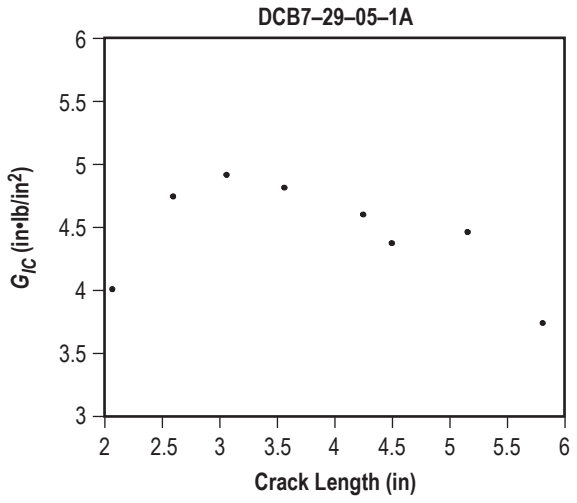
DCB7–29–05–1A
G_{IC} (in•lb/in^2)
Crack Length (in)

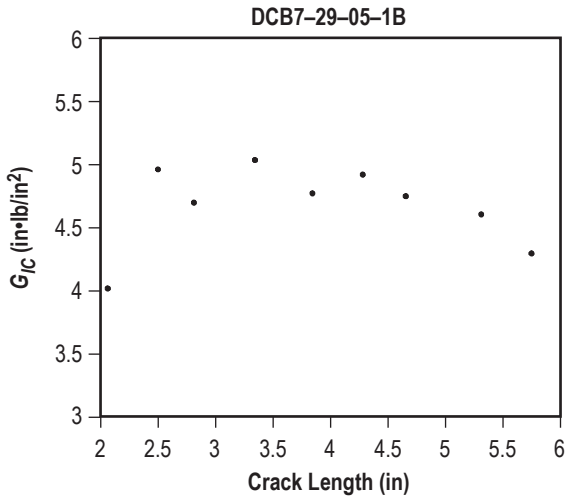
DCB7–29–05–1B
G_{IC} (in•lb/in^2)
Crack Length (in)

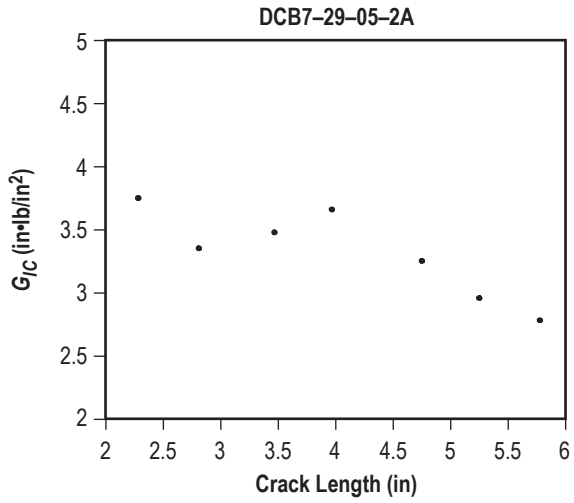
DCB7–29–05–2A
G_{IC} (in•lb/in^2)
Crack Length (in)

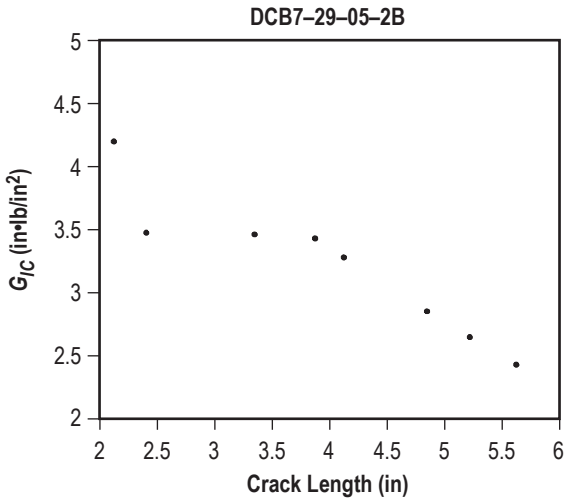
DCB7–29–05–2B
G_{IC} (in•lb/in^2)
Crack Length (in)

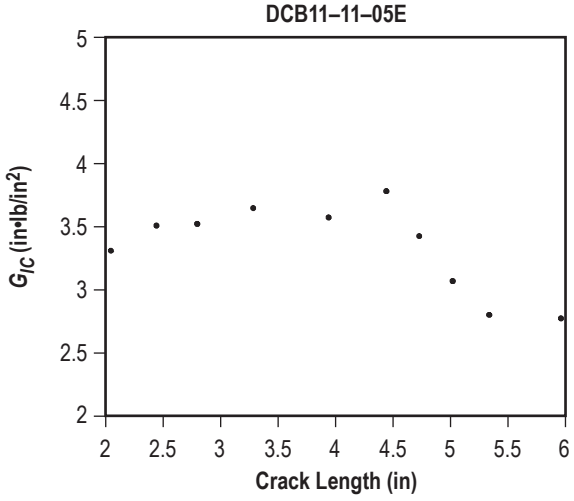
DCB11–11–05E
G_{IC} (in•lb/in^2)
Crack Length (in)

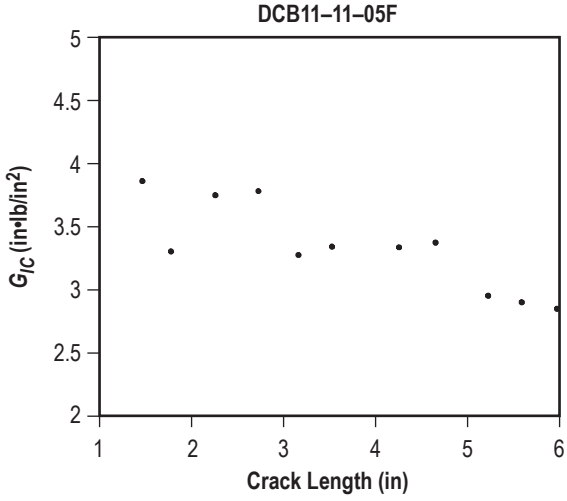
DCB11–11–05F
G_{IC} (in•lb/in^2)
Crack Length (in)

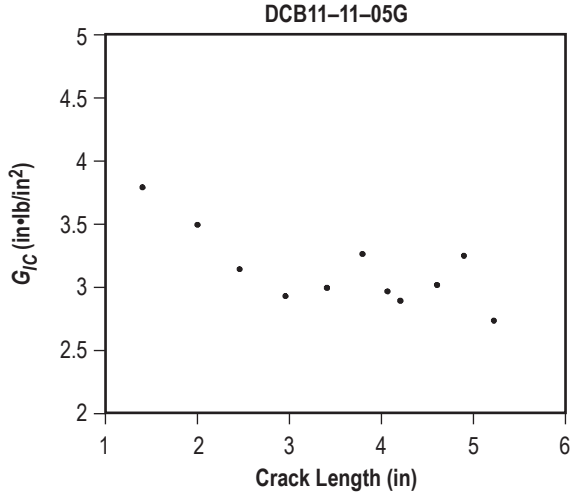
DCB11–11–05G
G_{IC} (in•lb/in^2)
Crack Length (in)

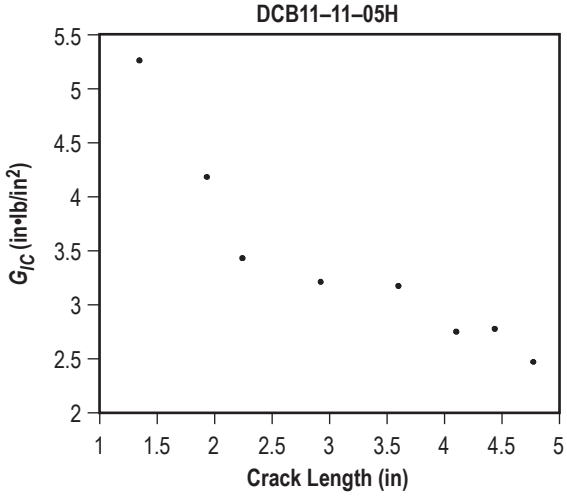
DCB11–11–05H
G_{IC} (in•lb/in^2)
Crack Length (in)

APPENDIX D—DATA FROM THE DOUBLE CANTILEVER BEAM TESTS WITHOUT STIFFENERS

Plots used to generate nonstiffened specimen data.

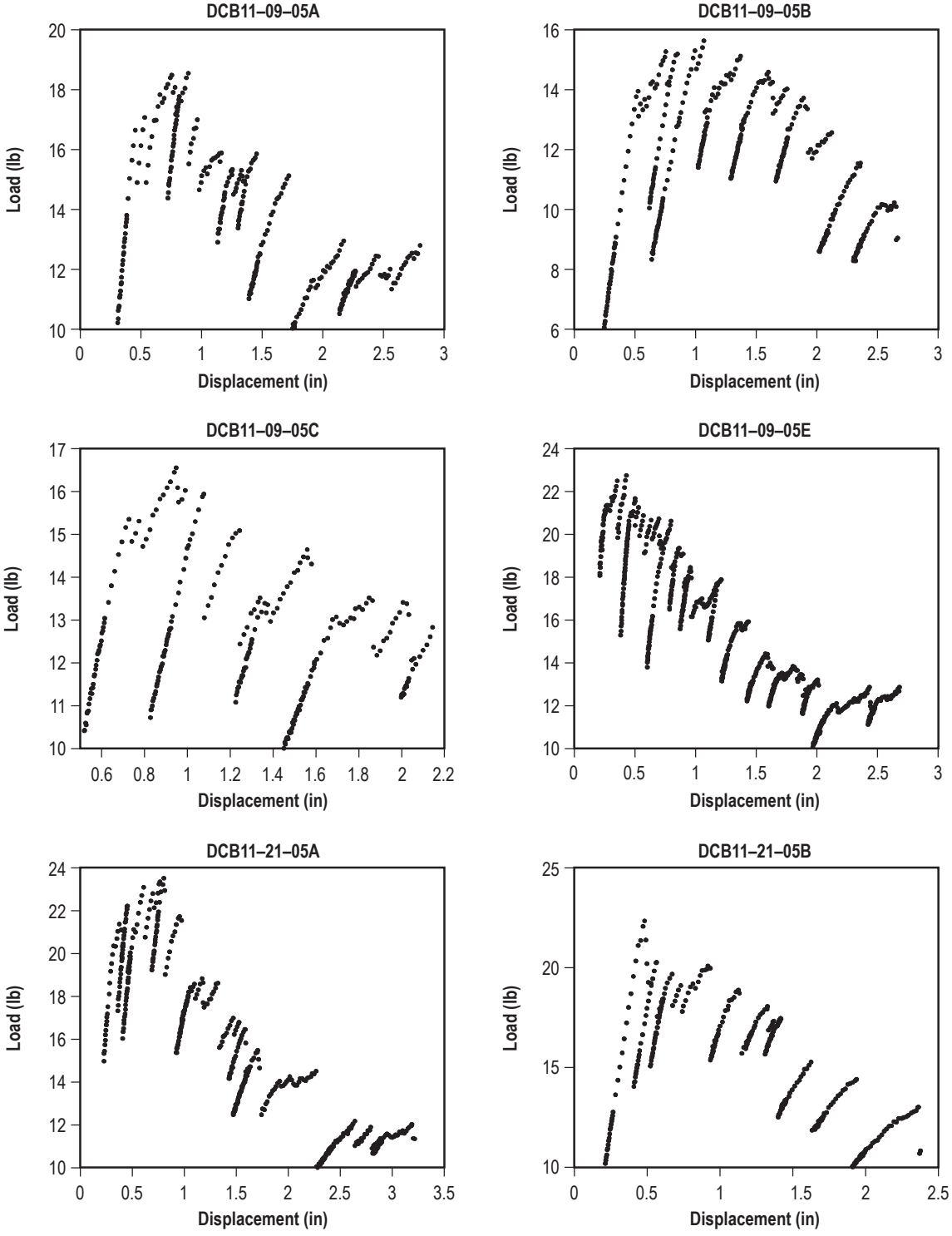

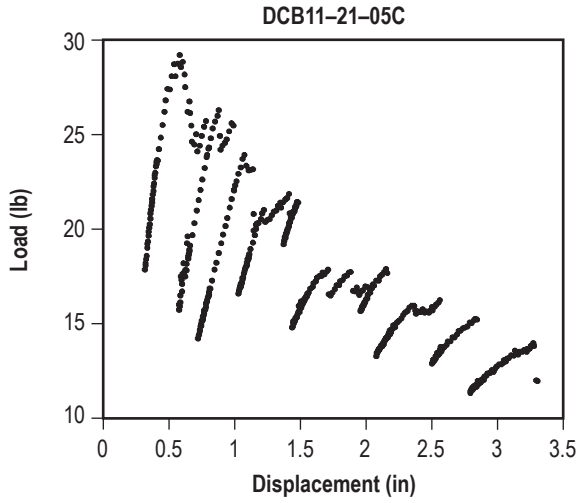
DCB11–21–05C
Load (lb)
Displacement (in)
30
25
20
15
10
0
0.5
1
1.5
2
2.5
3
3.5

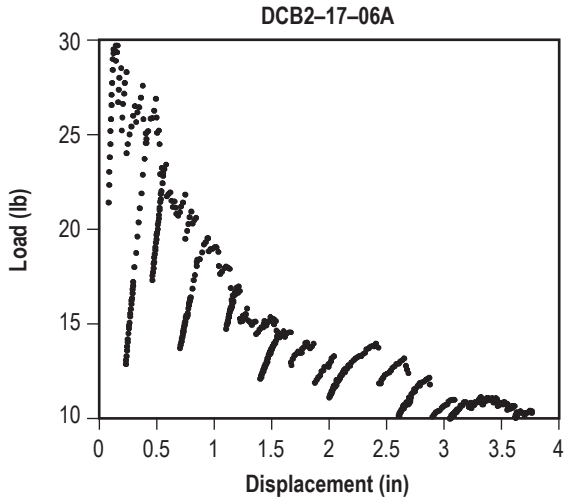
DCB2–17–06A
Load (lb)
Displacement (in)
30
25
20
15
10
0
0.5
1
1.5
2
2.5
3
3.5
4

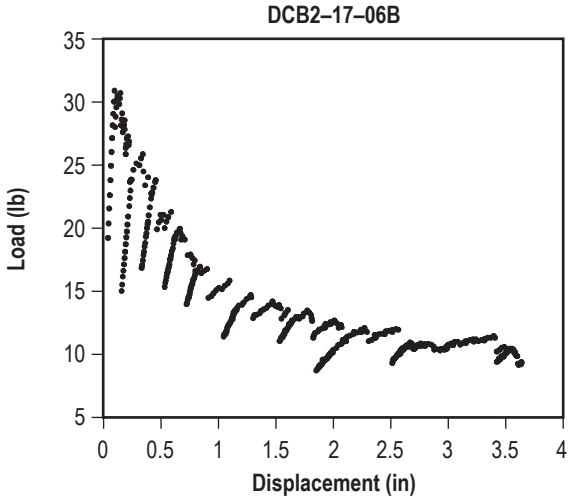
DCB2–17–06B
Load (lb)
Displacement (in)
35
30
25
20
15
10
5
0
0.5
1
1.5
2
2.5
3
3.5
4

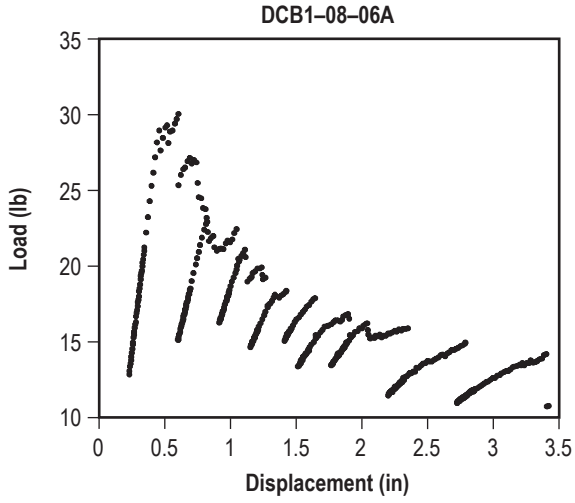
DCB1–08–06A
Load (lb)
Displacement (in)
35
30
25
20
15
10
0
0.5
1
1.5
2
2.5
3
3.5

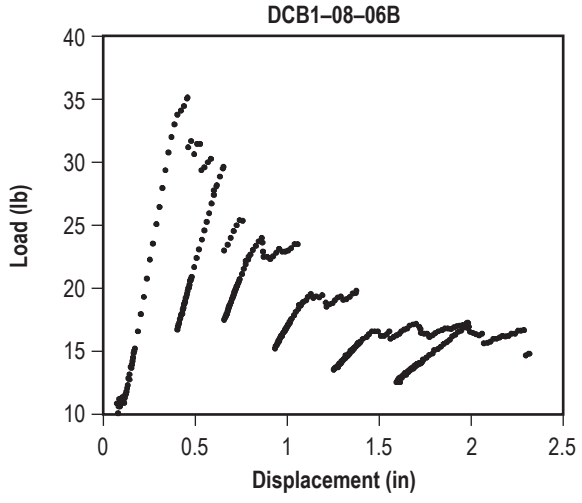
DCB1–08–06B
Load (lb)
Displacement (in)
40
35
30
25
20
15
10
0
0.5
1
1.5
2
2.5

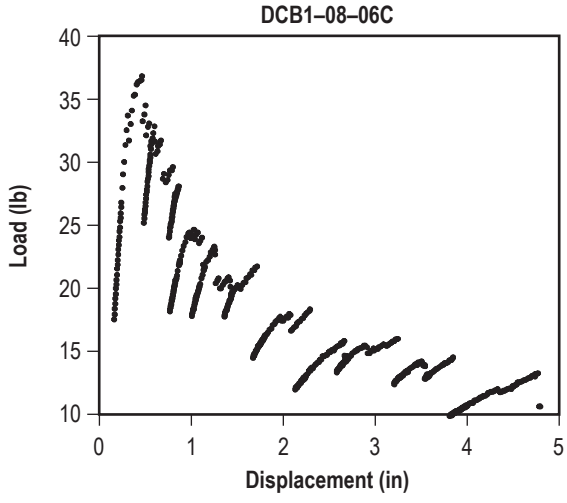
DCB1–08–06C
Load (lb)
Displacement (in)
40
35
30
25
20
15
10
0
1
2
3
4
5

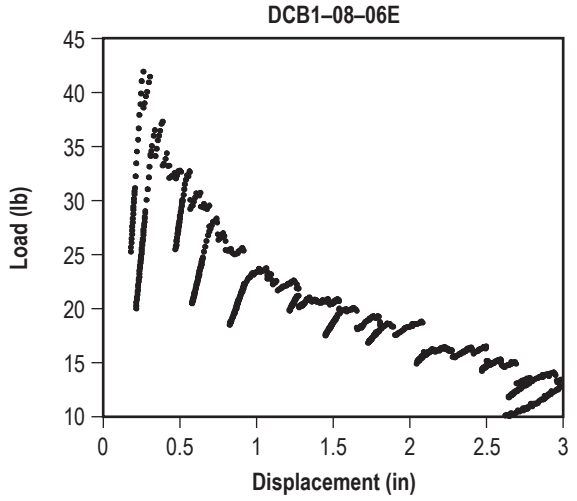
DCB1–08–06E
Load (lb)
Displacement (in)
45
40
35
30
25
20
15
10
0
0.5
1
1.5
2
2.5
3

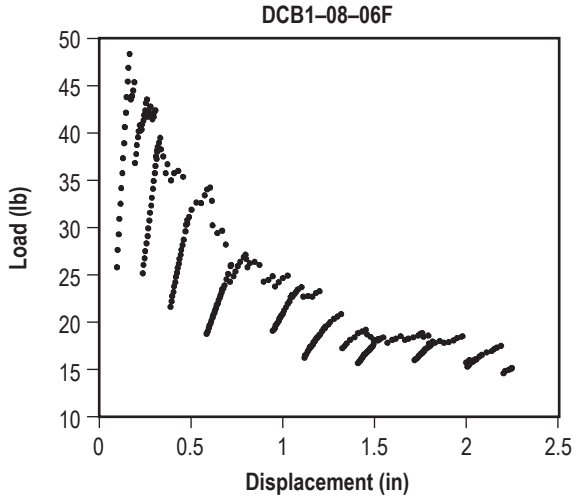
DCB1–08–06F
Load (lb)
Displacement (in)
50
45
40
35
30
25
20
15
10
0
0.5
1
1.5
2
2.5

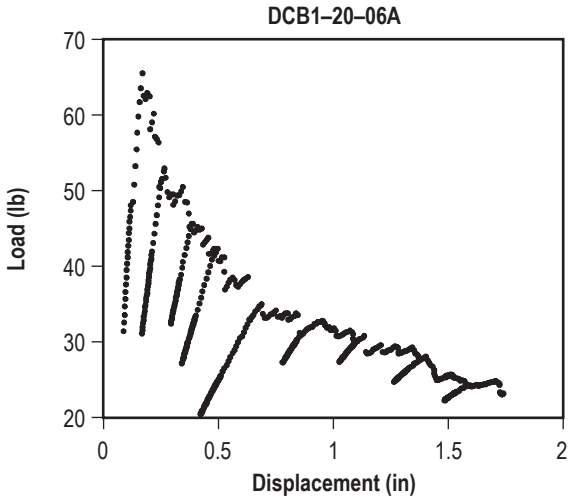
DCB1–20–06A
Load (lb)
Displacement (in)
70
60
50
40
30
20
0
0.5
1
1.5
2

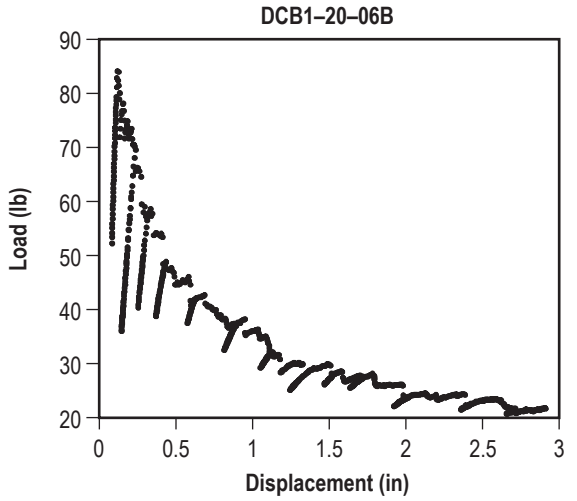
DCB1–20–06B
Load (lb)
Displacement (in)
90
80
70
60
50
40
30
20
0
0.5
1
1.5
2
2.5
3

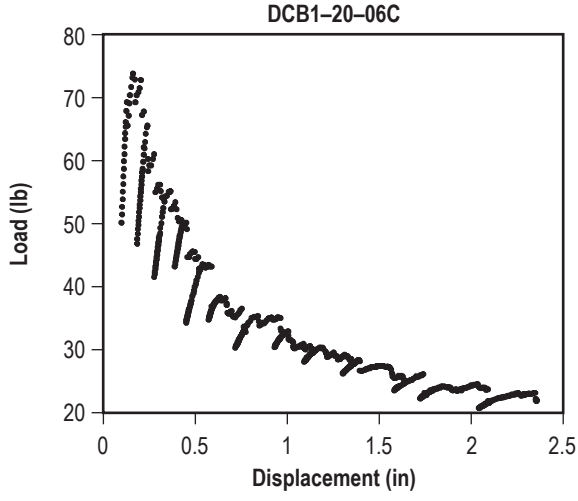
DCB1–20–06C
Load (lb)
Displacement (in)
80
70
60
50
40
30
20
0
0.5
1
1.5
2
2.5

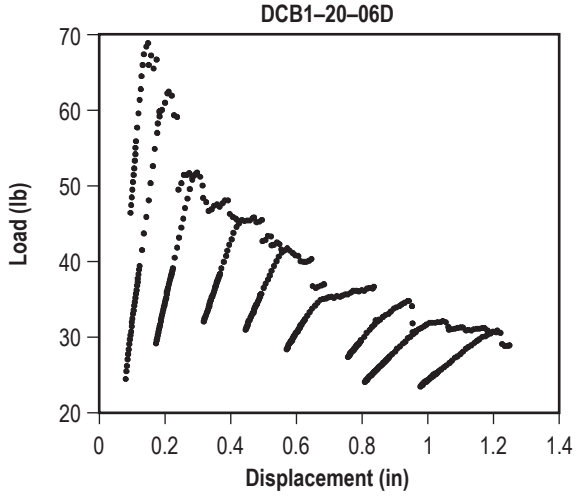
DCB1–20–06D
Load (lb)
Displacement (in)
70
60
50
40
30
20
0
0.2
0.4
0.6
0.8
1
1.2
1.4

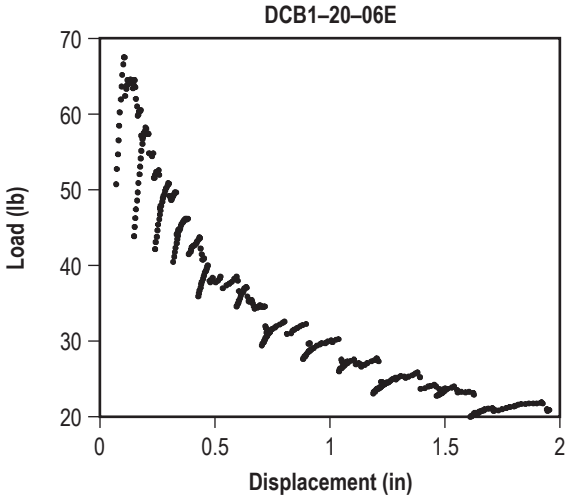
DCB1–20–06E
70
60
50
40
30
20
Load (lb)
0
0.5
1
1.5
2
Displacement (in)

APPENDIX E—R-CURVES FOR THE DOUBLE CANTILEVER BEAM TESTS WITHOUT STIFFENERS

Plots used to generate R-curves for the nonstiffened specimens.

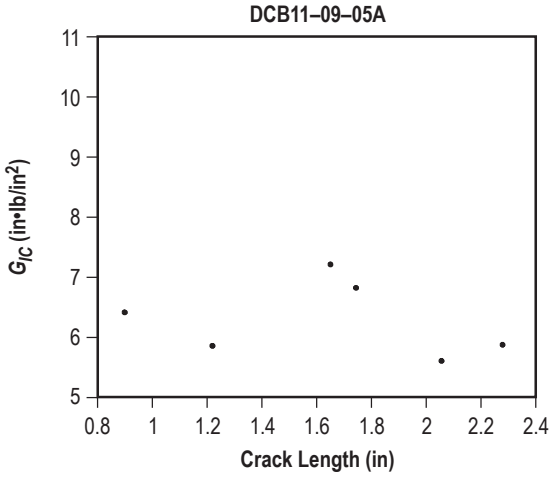

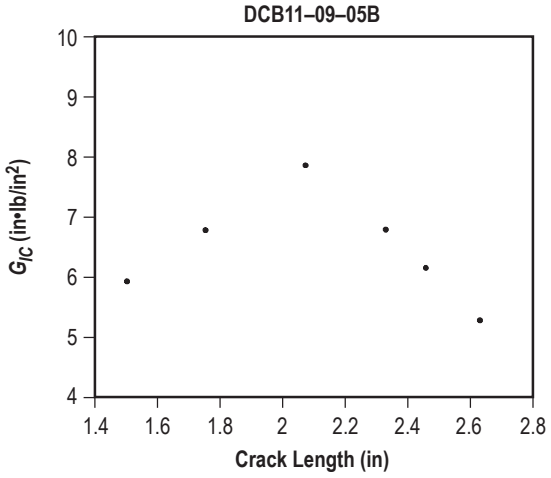

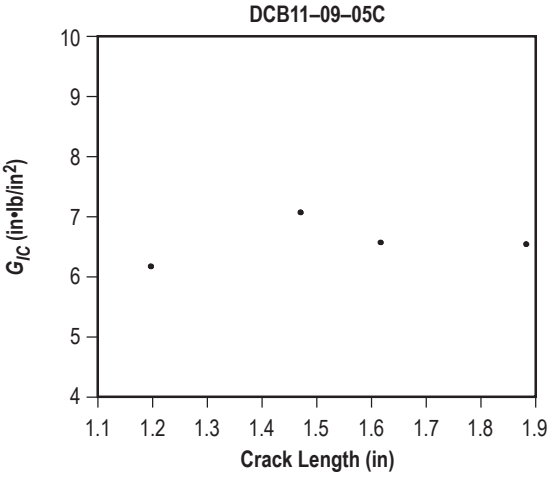

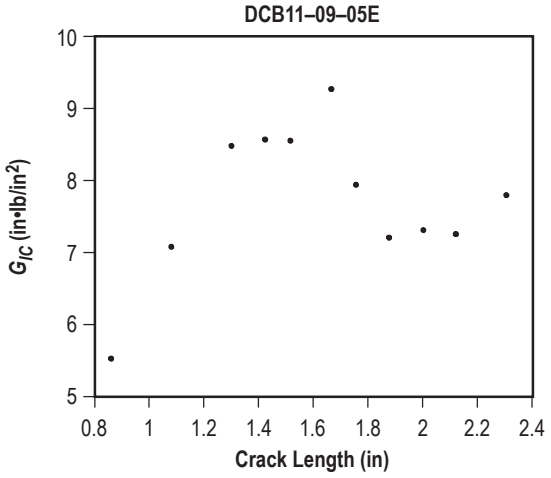

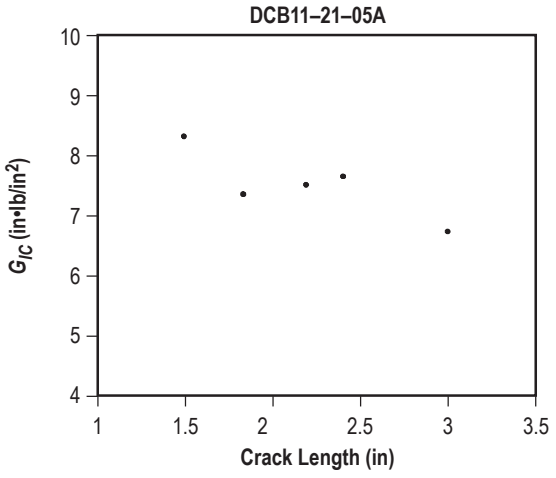

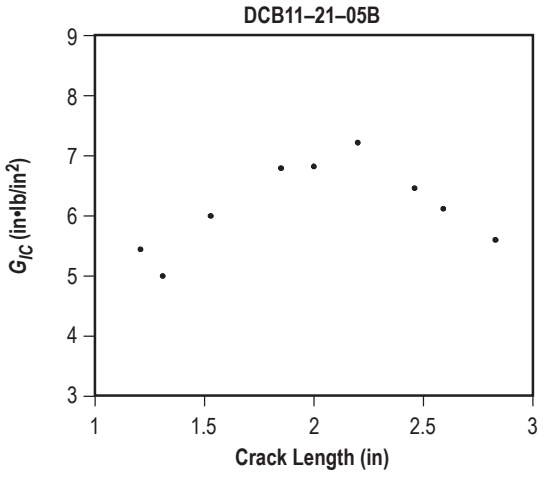

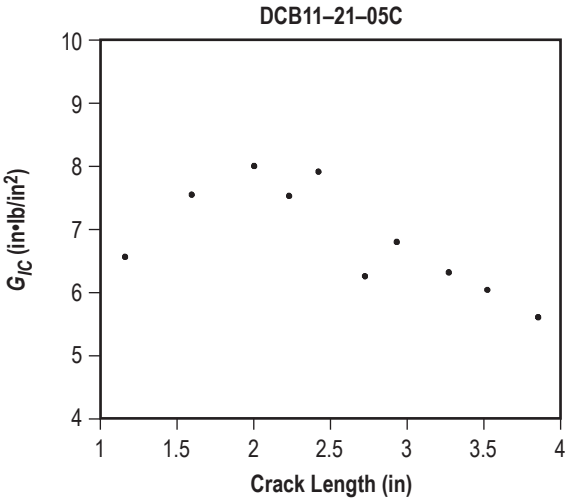
DCB11–21–05C
G_{IC} (in•lb/in^2)
Crack Length (in)

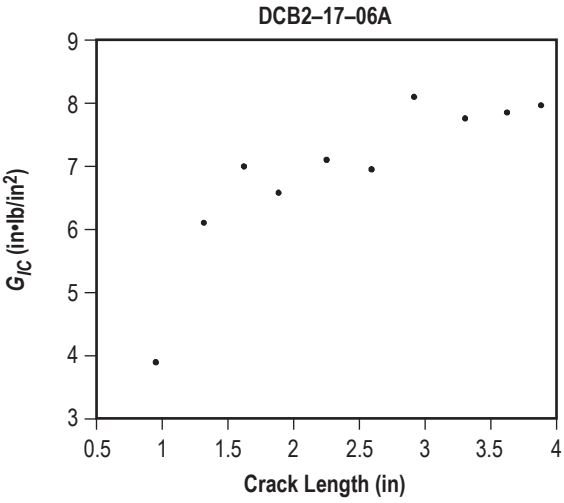
DCB2–17–06A
G_{IC} (in•lb/in^2)
Crack Length (in)

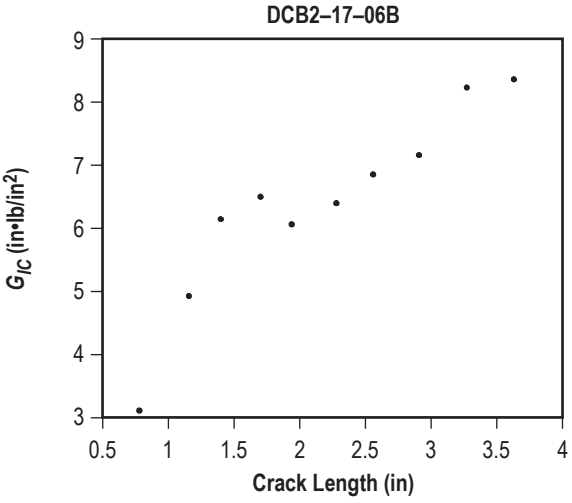
DCB2–17–06B
G_{IC} (in•lb/in^2)
Crack Length (in)

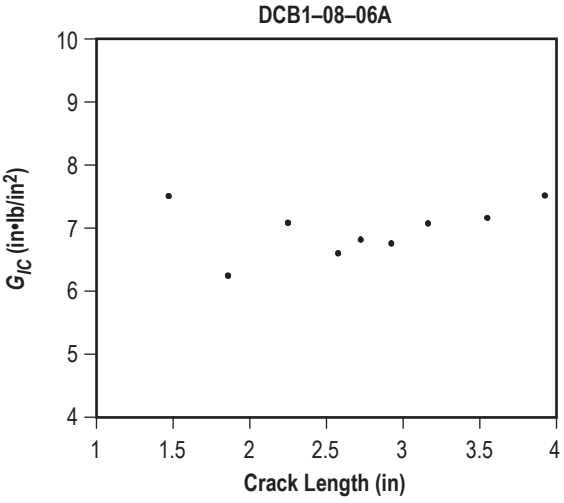
DCB1–08–06A
G_{IC} (in•lb/in^2)
Crack Length (in)

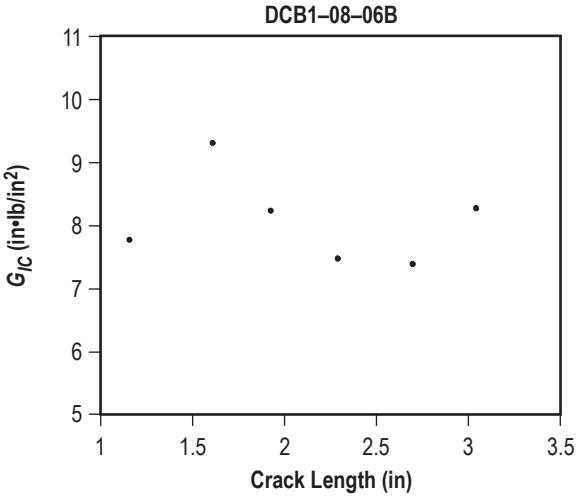
DCB1–08–06B
G_{IC} (in•lb/in^2)
Crack Length (in)

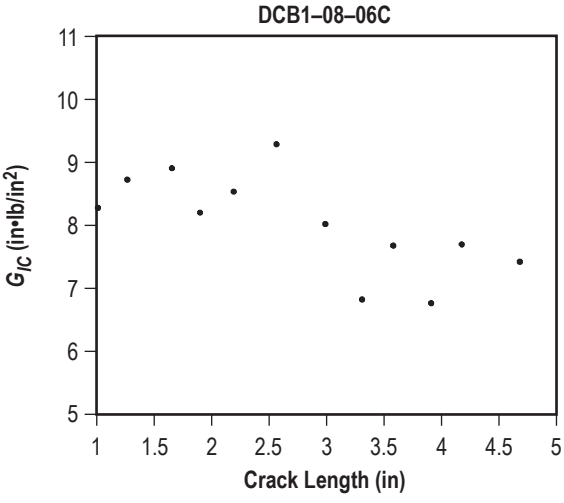
DCB1–08–06C
G_{IC} (in•lb/in^2)
Crack Length (in)

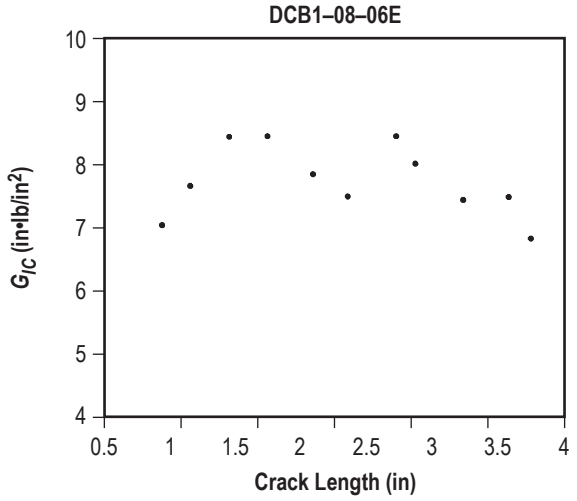
DCB1–08–06E
G_{IC} (in•lb/in^2)
Crack Length (in)

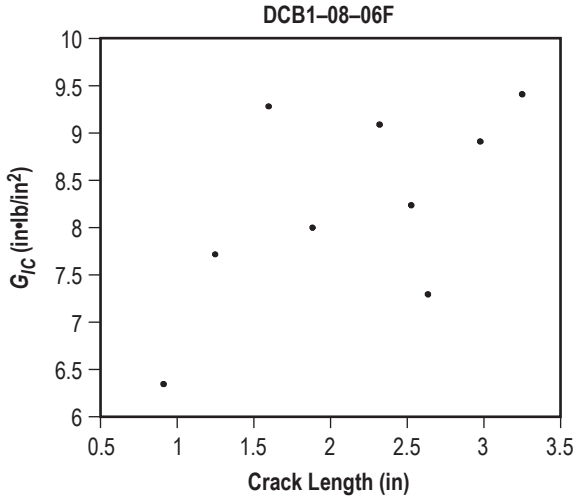
DCB1–08–06F
G_{IC} (in•lb/in^2)
Crack Length (in)

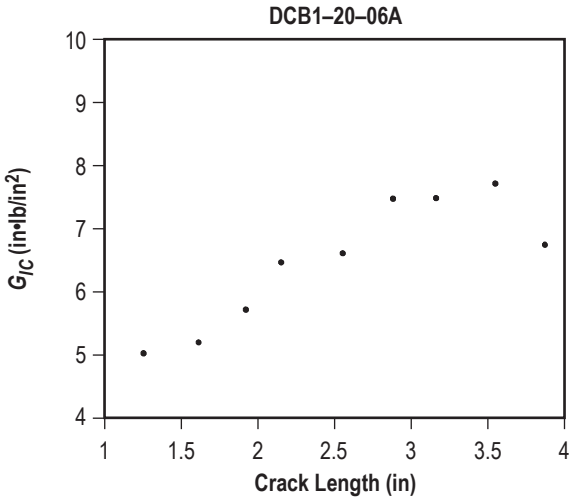
DCB1–20–06A
G_{IC} (in•lb/in^2)
Crack Length (in)

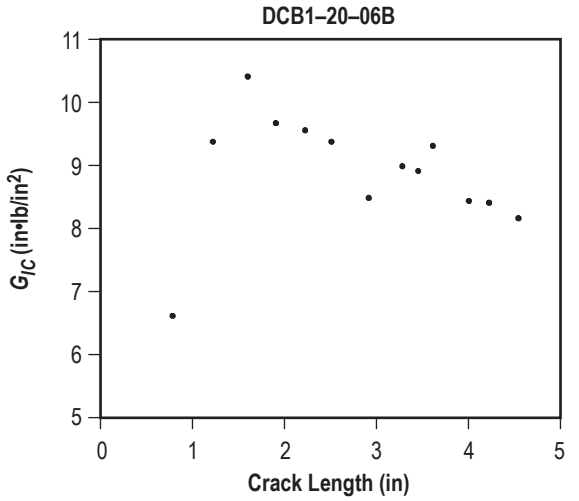
DCB1–20–06B
G_{IC} (in•lb/in^2)
Crack Length (in)

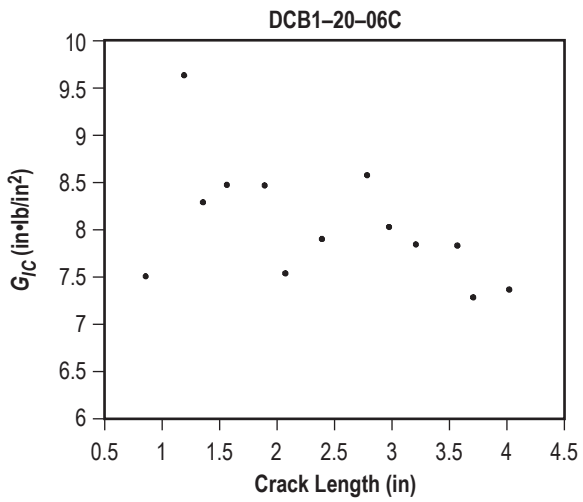
DCB1–20–06C
G_{IC} (in•lb/in^2)
Crack Length (in)

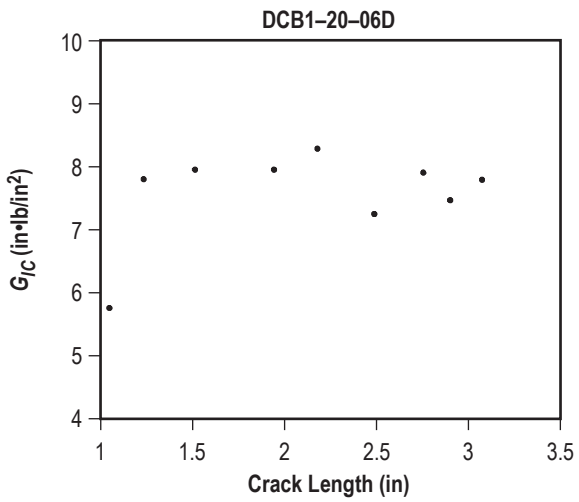
DCB1–20–06D
G_{IC} (in•lb/in^2)
Crack Length (in)

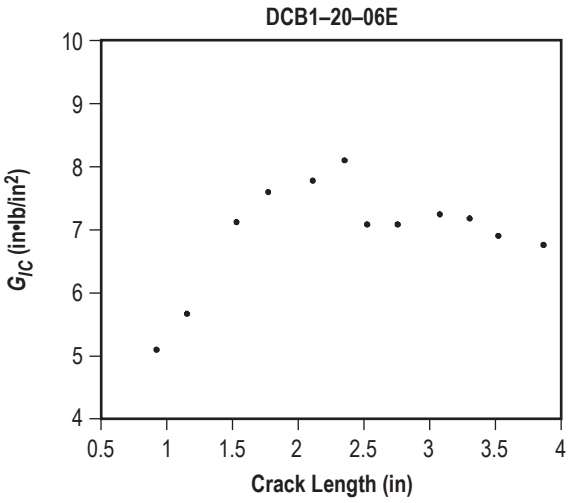
DCB1–20–06E
10
9
8
7
6
5
4
G_{IC} (in•lb/in^2)
0.5
1
1.5
2
2.5
3
3.5
4
Crack Length (in)

REFERENCES

1. Final Report of the X–33 Liquid Hydrogen Tank Test Investigation Team, NASA, Marshall Space Flight Center, May 2000.

2. Ko, W.L.: "Open-Mode Debonding Analysis of Curved Sandwich Panels Subjected to Heating and Cryogenic Cooling on Opposite Faces," NASA TP—1999–206580, 1999.

3. Ko, W.L.: "Debonding Stress Concentrations in a Pressurized Lobed Sandwich-Walled Generic Cryogenic Tank," NASA TP—2004–212849, 2004.

4. Peck, S.O.: "Lecture Notes: Honeycomb Sandwich Structures I and II," UCLA Extension, 2002.

5. Olsson, K.-A.; and Lonno, A.: "Shear Fatigue of the Core and Peeling of Skins in GRP-Sandwich," Proceedings of the Third International Conference on Marine Applications of Composite Materials, March 19–21, Melbourne, FL, 1990.

6. Grenestedt, J.L.: "Development of a New Peel Stopper for Sandwich Structures," *Composites Science and Technology*, Vol. 61, No. 11, pp. 1555–1559, August 2001.

7. Okada, R.; and Kortschot, M.T.: "The Role of the Resin Fillet in the Delamination of Honeycomb Sandwich Structures," *Composites Science and Technology*, Vol. 62, No. 14, pp. 1811–1819, November 2002.

8. Prasad, S.; and Carlsson, L.A.: "Debonding and Crack Kinking in Foam Core Sandwich Beams-II Experimental Investigation," *Engineering Fracture Mechanics*, Vol. 47, No. 6, pp. 825–841, 1994.

9. Cantwell, W.J.; and Davies, P.: "A Study of Skin-Core Adhesion in Glass Fibre Reinforced Sandwich Materials," *Applied Composite Materials*, Vol. 3, No. 6, pp. 407–420, November 1996.

10. Ural, A.; Zehnder, A.T.; and Ingreffea, A.R.: "Fracture Mechanics Approach to Facesheet Delamination in Honeycomb: Measurement of Energy Release Rate of the Adhesive Bond," *Engineering Fracture Mechanics*, Vol. 70, pp. 93–103, 2003.

11. Liechti, K.M.; and Martin, B.: "Delamination of a High-Temperature Sandwich Plate," *Experimental Mechanics*, Vol. 42, No. 2, pp. 206–213, June 2002.

12. Papanicolaou, G.C.; and Bakos, D.: "Effect of Treatment Conditions on the Mode I Delamination Fracture Toughness of Sandwich Structures," *Journal of Composite Materials*, Vol. 29, No. 17, pp. 2295–2316, 1995.

13. Berkowitz, C.K.; and Johnson, W.S.: "Fracture and Fatigue Tests and Analysis of Composite Sandwich Structure," *Journal of Composite Materials*, Vol. 39, No. 16, pp. 1417–1431, 2005.

14. Gates, T.S.; and Herring, H.M.: "Facesheet Push-off Tests to Determine Composite Sandwich Toughness at Cryogenic Temperatures," Proceedings 42nd AIAA/ASME/ASCE/AHS/ASC Structures, Structural Dynamics, and Materials Conference and Exhibit, Seattle, WA, April 16–19, 2001.

15. Cantwell, W.J.; Scudamore, R.; Ratcliffe, J.; and Davies, P.: "Interfacial Fracture in Sandwich Laminates," *Composites Science and Technology*, Vol. 59, No. 14, pp. 2079–2085, 1999.

16. Devitt, D.F.; Schapery, R.A.; and Bradley, W.L.: "A Method for Determining the Mode I Delamination Fracture Toughness of Elastic and Viscoelastic Composite Materials," *Journal of Composite Materials*, Vol. 14, pp. 270–285, 1980.

17. Reeder, J.R.; Demarco, K.; and Whitley, K.S.: "The Use of Doublers in Delamination Toughness Testing," Proceedings of the American Society for Composites 17th Technical Conference, 2002.

REPORT DOCUMENTATION PAGE

Form Approved
OMB No. 0704-0188

1. AGENCY USE ONLY *(Leave Blank)*	2. REPORT DATE	3. REPORT TYPE AND DATES COVERED
	December 2006	Technical Publication

4. TITLE AND SUBTITLE
Measuring Core/Facesheet Bond Toughness in Honeycomb Sandwich Structures

5. FUNDING NUMBERS

6. AUTHORS
A.T. Nettles

7. PERFORMING ORGANIZATION NAME(S) AND ADDRESS(ES)
George C. Marshall Space Flight Center
Marshall Space Flight Center, AL 35812

8. PERFORMING ORGANIZATION REPORT NUMBER
M–1180

9. SPONSORING/MONITORING AGENCY NAME(S) AND ADDRESS(ES)
National Aeronautics and Space Administration
Washington, DC 20546–0001

10. SPONSORING/MONITORING AGENCY REPORT NUMBER
NASA/TP—2006–214713

11. SUPPLEMENTARY NOTES
Prepared by Materials Processes and Manufacturing Department, Engineering Directorate

12a. DISTRIBUTION/AVAILABILITY STATEMENT
Unclassified-Unlimited
Subject Category 24
Availability: NASA CASI 301–621–0390

12b. DISTRIBUTION CODE

13. ABSTRACT *(Maximum 200 words)*

This study examines two test methods to evaluate the peel toughness of the skin to core debond of sandwich panels. The methods tested were the climbing drum (CD) peel test and the double cantilever beam (DCB) test. While the CD peel test is only intended for qualitative measurements, it is shown in this study that qualitative measurements can be performed and compare well with DCB test data. It is also shown that artificially stiffening the facesheets of a DCB specimen can cause the test to behave more like a flatwise tensile test than a peel test.

14. SUBJECT TERMS
sandwich structures, mode I, honeycomb, fracture toughness

15. NUMBER OF PAGES
64

16. PRICE CODE

17. SECURITY CLASSIFICATION OF REPORT	18. SECURITY CLASSIFICATION OF THIS PAGE	19. SECURITY CLASSIFICATION OF ABSTRACT	20. LIMITATION OF ABSTRACT
Unclassified	Unclassified	Unclassified	Unlimited

National Aeronautics and
Space Administration
IS20
George C. Marshall Space Flight Center
Marshall Space Flight Center, Alabama
35812